Instructions to Finite Element Simulation of Butt-welded High-Strength Steel Joints

Finite Element Simulations using Abaqus CAE

Construction Engineering		Abstract
Author	Robert Tihhomirov	Year 2024
Subject	Instructions to Finite Element Simulation of Butt-welded High-Strength Steel Joints. Finite Element Simulations Using Abaqus CAE	
Supervisors	Blerand Greiçevci, Jarmo Havula	

This bachelor's thesis, which has been commissioned by HAMK Tech, a research unit within Häme University of Applied Sciences, is a part of a larger research project focused on high-strength steel applications and welded connections. The primary objective of this thesis is to understand the main features of Abaqus CAE and provide valid instructions on how to use software for the simulation of the butt-welded tensile test specimen S700 with a thickness of 4 mm. This thesis builds upon previous research and tensile experiments executed in HAMK Tech laboratories.

The goals of this thesis are to describe the steps of modeling with Abaqus, and the calculations required using the test results received from HAMK Tech. The thesis includes various example models and the description of the modeling process. The modeling process includes several key tasks such as defining geometry, specifying key parameters, and defining the valid input data for material properties. Previous bachelor's theses serve as valuable sources, contributing to the continuity of the research.

Significant advancements have been made in this thesis, particularly in the areas of reducing the simulation time and defining the input data. The created models depict the realistic failure mechanism of the specimen and provide valid output data as force-displacement and stress-strain curves.

Keywords	High strength steel, FEM simulation, Abaqus
Pages	42 pages and appendices 23 pages

List of symbols and abbreviations

HAZ   Heat affected zone

BM   Base material

WM   Weld material

HSS   High strength steel

UTS   Ultimate tensile strength

FEM   Finite element method

σ_{true} True tensile stress

σ_{eng} Engineering tensile stress

ε_{true} True tensile strain

ε_{eng} Engineering tensile strain

ε_{pl} Logarithmic plastic strain

E   Modulus of Elasticity

G_f Fracture energy

L Characteristic element length

ε^{pl} Fracture strain

σ_y Engineering stress

V Volume of one mesh element

A The largest face area of the mesh element

Content

Figures, tables, and equations

Appendices

1 Introduction

HSS is a significant advancement in the use of structural steel, offering benefits such as weight reduction, increased load-carrying capacity, cost efficiency, etc (Hajro, 2017, p. 0611). However, there are still some uncertainties in the behavior of high-strength steel, as it is not sufficiently researched and covered in standards. Regarding high-strength steel, the main uncertainty is the welding process (Nguyen, 2018). In comparison with mid-steel weldments, welded HSS elements have a higher strength-weight ratio that leads to reduced material consumption (Havula et al., 2018). Despite this, owing to the insufficient research and understanding of this new material, this led to many restrictions on using high-strength steel welded joints in structures, as incorrect welding parameters could weaken the weld joint, particularly in the HAZ.

One approach to address this issue is through regular physical experiments on HSS in the laboratory that would contribute to the solution by providing valuable data and insights into the behavior of HSS. However, this form of testing tends to be costly and unsustainable. Hence, it is necessary to reconsider this conventional testing method and widen the physical experiments with computational testing simulations. By developing an accurate finite element model that incorporates realistic material properties, it becomes accessible to create new testing simulations for various materials. Consequently, the substantial expenses associated with physical testing can be minimized, as the behavior and mechanisms of the tests can be partially predicted through finite element simulations.

Therefore, this thesis aims to contribute to this new approach by investigating the ways to work with finite element model in Abaqus software and apply its features to run the simulations of the tensile experiments. To assist this approach, the research on this topic is implemented in cooperation with other research projects and laboratory experiments done in HAMK Tech.

2 Objective

The objective of this thesis is to understand the main features of Abaqus and provide valid instructions on how to use the software for simulation of the tensile experiments for High-Strength Steels. Moreover, it aims to show how to work with data received from the experiments and use it as input data for the model.

2.1 Background study

This thesis is a part of the larger research project conducted in HAMK Tech which is doing multiple studies on high-strength steel weldments and mechanical properties of heat-affected zones. Therefore, this thesis encompasses several studies that have been conducted previously. For instance, Nguyen (2018) performed research on the effects of heat input and different amounts of weld runs on the mechanical properties of butt-welded steel joints. Ngo's thesis (2021) was a direct continuation of Pham Nguyen's (2018) thesis and focused on creating the finite element model of an S500 specimen to run the simulation using LS-Dyna as the main FEM software. Rahman (2022) aimed to study the mechanical properties of S700 steel weldments with two different heat inputs and conducted tensile tests focusing on comparing the mechanical properties of weldments and base materials.

Despite these previous studies and other studies conducted before, there is still a gap in the research when it comes to modelling using Abaqus, since previous studies do not provide clear instructions on how to create the model for tensile experiment and how to process the data of the experiment for material input in Abaqus. Therefore, to fill these gaps, this thesis aims to depict the entire process of modelling and working with experimental data in an illustrative and clear way. All the experimental work listed in this thesis was carried out by HAMK Tech staff, and HAMK Tech provided the material data for the simulations done in this thesis.

2.2   Research questions

The research process of this thesis involves a recreation of a tensile testing specimen of high-strength steel S700 with Abaqus as the main FEM software. The finite element model must represent an accurate geometry of the testing specimen and contain different zones such as base metal (BM), weld metal (WM), and heat-affected zone (HAZ). This thesis aims to simulate the specimen's tensile experiment and receive stress-strain graphs for all three material models nearly identical to the graphs received from the laboratory, as well as force-displacement curve that would resemble similar pattern. To accomplish that, thesis aims to answer following research questions:

- What are the relevant input data to simulate the finite element analysis of welded tensile test?
- What features of Abaqus need to be used in the modeling of the tensile specimen?
- How to evaluate the accuracy of the simulation?

2.3   Limitations

The scope of this thesis is limited to a singular welded tensile specimen, comprising two 4 mm thick HSS plates with a nominal yield strength of 700 MPa. Utilizing Abaqus, simulations were carried out using a model specifically customized for this specimen. It is important to note that the thesis does not delve into the precise representation of material failure beyond the UTS point, nor does it encompass a comprehensive verification and validation procedure for the finite element analysis. Instead, the primary emphasis lies on elucidating the modeling process of the specimen, offering practical examples and insights into effective modeling techniques.

2.4 Thesis framework

Figure 1 depicts the framework adhered to throughout the entire thesis study. The process began with an investigation into materials relevant to finite element modeling. Concurrently, the preparation of the specimen and subsequent testing took place at the HAMK Tech laboratory. Following the receipt of test results, these values were converted into the necessary input data. Subsequently, the model underwent several adjustments until the simulation ran smoothly and accurately.

Figure 1 Thesis framework illustration
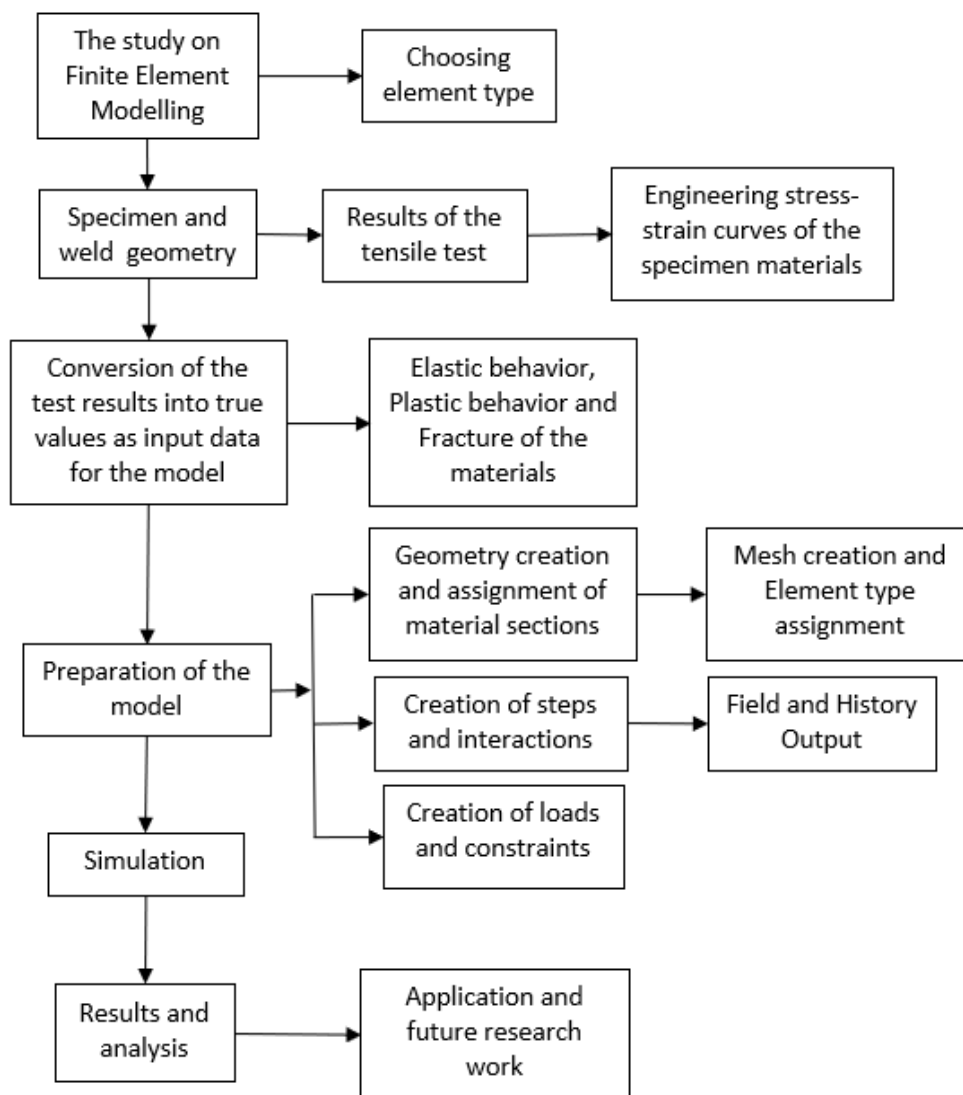
3   Literature review

This chapter delves into the transformative effects of welding on material microstructure, emphasizing the critical role of the HAZ in shaping mechanical properties. Furthermore, it explores Finite Element Modelling considerations, ensuring a balance between accuracy and computational efficiency for modeling solid structures in welding applications.

3.1   The microstructure of the welding joint and HAZ

As the heat source interacts with the material, the impact of the thermal variations on the material differs across different regions. Consequently, a heterogeneous microstructure forms in the welded joint. Mechanical properties exhibit variations from one zone to another, influenced not only by the heat input but also by the filler material. Broadly speaking, a welded joint can be divided into three distinct zones: the fusion zone (FZ), the partially melted zone (PMZ), and the heat-affected zone (HAZ) (Peltonen, 2014, p. 27). Figure 2 provides a schematic presentation of different zones at the welded joint.

Figure 2. Different zones at the welded joint (Peltonen, 2014, p. 27).
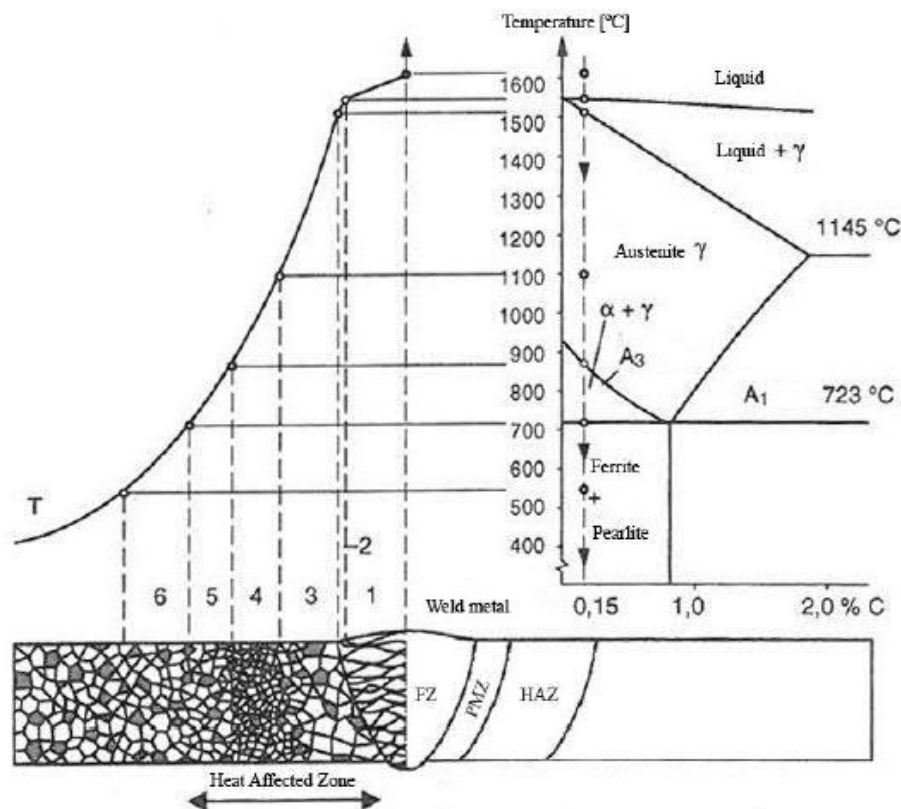
The HAZ is the region of the material surrounding the weld where the microstructure has been altered due to the heating and cooling cycles experienced during welding. This thermal cycle is causing irregularity to the material in which case the joint is the weakest link of the structure (Peltonen, 2014, p. 26). The microstructure of the HAZ can have a significant impact on the mechanical properties of the welded joint, such as strength and toughness. The rapid heating and subsequent cooling of the material during welding can lead to the formation of different microstructures in the HAZ. One of the most significant changes that occur in the HAZ is the transformation of austenite to different phases such as ferrite, bainite, or martensite, depending on the cooling rate.

Based on microstructural changes caused by welding, the heat-affected zone (HAZ) can be divided into several regions:

- CGHAZ (Coarse-grained heat-affected zone) is located next to the fusion zone (FZ) or welding material (WM), which is exposed to high temperatures of around 1200-1500 ºC. The grain size of austenite in this zone increases due to coarsening, resulting in a reduction of precipitations that constrain grain growth.

- FGHAZ (Fine-grained heat-affected zone) is the region adjacent to the CGHAZ, where the grain size of austenite is smaller than in the CGHAZ. The zone is exposed to high temperatures of around A3 - 1200 ºC, resulting in the formation of ferritic phases during cooling. The homogenization of austenite is not carried out perfectly, leading to a higher fraction of hardening ferritic structures. Transformation to martensite may occur due to the enriched carbon concentration of retained austenite.

- ICHAZ (Inter-critical heat-affected zone) is partially austenized and exposed to a temperature range around A1-A3. The carbon-enriched austenite in this zone can lead to the formation of hard ferritic structures like martensite if the cooling rate is high.

- SCHAZ (Subcritical heat-affected zone) is the outer part of the HAZ, exposed to temperatures below A1

The CGHAZ is the most critical zone within the heat-affected zone considering the Charpy impact strength and the FGHAZ is the most critical in consideration of tensile strength, furthermore these are weakest links in the entire welding joint. In the finite element model of this thesis, the heat-affected zones are assumed to be one region with uniform material

properties, mainly representing the properties of CGHAZ and FGHAZ. In future continuation of this research a more detailed heat-affected zone can be applied to the finite element model.

3.2 Relationship between heat input and cooling time

The heat input in welding is defined as the amount of energy applied to the welded joint per unit length. It is typically controlled by adjusting the welding current and voltage, as well as the welding speed. The heat input affects the cooling rate of the weld, which, in turn, determines the microstructure of the welded joint.

The cooling time is a critical parameter that influences the microstructure and mechanical properties of the WM, HAZ and BM. The cooling time represents the time it takes for the welded joint to cool down from 800 ºC to 500 ºC. The cooling time depends on several factors, including the welding process, the heat input, and the thickness of the material (Pirinen, 2013).

When a high heat input is used, the cooling time is longer, resulting in coarser microstructures in the weld metal and HAZ. In contrast, a low heat input leads to a shorter cooling time and finer microstructures. The cooling rate and cooling time also affect the formation of various phases in the welded joint, such as the formation of martensite and bainite.

Pirinen (2013) explains that the cooling rate and cooling time can also affect the risk of hydrogen-induced cracking in high-strength steel welds. A longer cooling time allows for more time for hydrogen to diffuse out of the welded joint, reducing the risk of cracking. However, a longer cooling time can also lead to increased susceptibility to cold cracking, especially in thick sections, due to the higher residual stresses. Moreover, in the article Pirinen (2013) provides examples of the heat input and cooling times suitable for various welding processes used high strength steels, such as gas metal arc welding (GMAW), flux-cored arc welding (FCAW), and submerged arc welding (SAW).

Peltonen (2014, pp. 20-22) provides a detailed analysis of the weldability of high strength steel and the challenges associated with the welding process. Peltonen (2014) highlights the difficulties encountered when welding high strength steel, which have contributed to the limited adoption of the practice.

One of the major challenges associated with welding high strength steel is the susceptibility to hydrogen-induced cracking. The presence of hydrogen in the weld zone can lead to the formation of microcracks that reduce the strength and toughness of the material. This problem

is further exacerbated by high heat input required for welding, which increases the likelihood of HIC.

Another difficulty associated with welding high strength steel is the formation of martensite in HAZ. The rapid cooling of the material during welding can lead to the transformation of austenite to martensite, which is a hard and brittle phase that reduces the toughness of the material. This can lead to a reduction in the ductility and toughness of the weld, making it more prone to fracture under stress.

Despite these challenges, there has been a growing interest in the use of HSS in structural applications due to its high strength-to-weight ratio and improved performance under extreme loads. However, the limited adoption of this practice can be attributed to the challenges related to welding high-strength steel. The need for specialized welding techniques and the potential for welding defects has limited the adoption of HSS in many applications.

3.3 Literature review on Finite Element Modelling

The document (Simulia, Getting Started with ABAQUS (v6.6). Finite Elements and Rigid Bodies. Finite Elements. Continuum Elements, n.d.) highlights the importance of choosing an appropriate element type for a particular problem, since different element types have varying levels of accuracy and computational efficiency. The document gives a clear overview on characterization of the elements that is used by Abaqus CAE including Family, Degree of freedom, Number of nodes, Formulation, and Integration. Each of these is identified by the unique name, such as T2D2, S4R, or C3D8. In particular, the C3D8 element is recommended for modelling solid structure, such as steel specimen used in tensile tests, since it is an eight-node brick element with three degrees of freedom per node. This element provides a sufficient balance between accuracy and computational efficiency for many solid mechanics problems.

4 Research methodology

The following section provides a comprehensive overview of the research workflow, outlining key components such as the preparation of tensile specimen and laboratory work methods that were conducted by technical staff at HAMK Tech laboratory. Subsequently, this section delves into the explanation of Abaqus features and utilization of experimental data.

4.1 Sample preparation for the laboratory experiment

The case chosen for this study is the butt-welded joint of two steel plates. The welding process involved welding plates with a thickness of 4 mm using GMAW (Gas Metal Arc Welding) /MAG (Metal Active Gas). The chosen gas for GMAW was Mison 18. Real-time cooling rate values were recorded during welding to investigate the impact of welding parameters. Welding was conducted at HAMK Tech laboratory in Riihimäki to test the entire setup for tensile testing with an extension meter and ARAMIS system. All tensile test specimens were then cut to the required shape using water cutting. To attain HAZ properties with more controlled cooling times t8/5, precise heat treatment was conducted.

The base material selected for welding in this study was Strenx 700 MC PLUS whose mechanical properties are provided in Table 1. Strenx 700MC Plus, a remarkable variant of the Strenx grade, offers outstanding characteristics in terms of bending and mechanical cutting. This unique grade accelerates the progress of designing and manufacturing advanced load-bearing equipment with exceptional performance. Its superior formability and remarkable impact toughness make it an ideal choice for demanding applications. (SSAB, 2023)

Table 1. Mechanical properties of Strenx 700 MC PLUS (SSAB, 2023).

Thickness (mm)	Yield Strength R_{EH} (MPa)	Tensile Strength R_M (MPa)	Elongation A_5 (Min %)	Min. inner bending radius for 90 ° bend
3.0 – 10.00	700	750-950	13	1.0 x t
10.00 – 12.00	700	750-950	13	1.0 x t

The filler material used for welding was OK Aristorod 89 with a wire diameter of 1mm. OK AristoRod 89 is a low-alloyed, chromium-nickel-molybdenum solid wire designed for Gas Metal Arc Welding applications in ultra-high tensile strength steels. It is also applicable in situations requiring high-impact strength at lower temperatures. The AristoRod 89 wires are more than suitable for operating at high currents ensuring disturbance free wire feeding and maintaining

a stable arc with minimal spatter. This is achieved through its distinctive Advanced Surface Characteristics ASC technology (ESAB, 2023). Its tensile properties are shown in Table 2.

Table 2. Tensile properties of the filler wire (ESAB, 2023).

Tensile Properties			
Testing Condition EN 80 Ar/20CO2 (M21)	Yield Strength	Tensile Strength	Elongation
As welded	920 MPa	940 MPa	18%

Figures 3 and 4 depict the initial representations of the base metal parts and the welding filler material utilized in the specimen. However, these figures do not encompass the comprehensive details of the HAZ or the precise measurements obtained after the welding process.

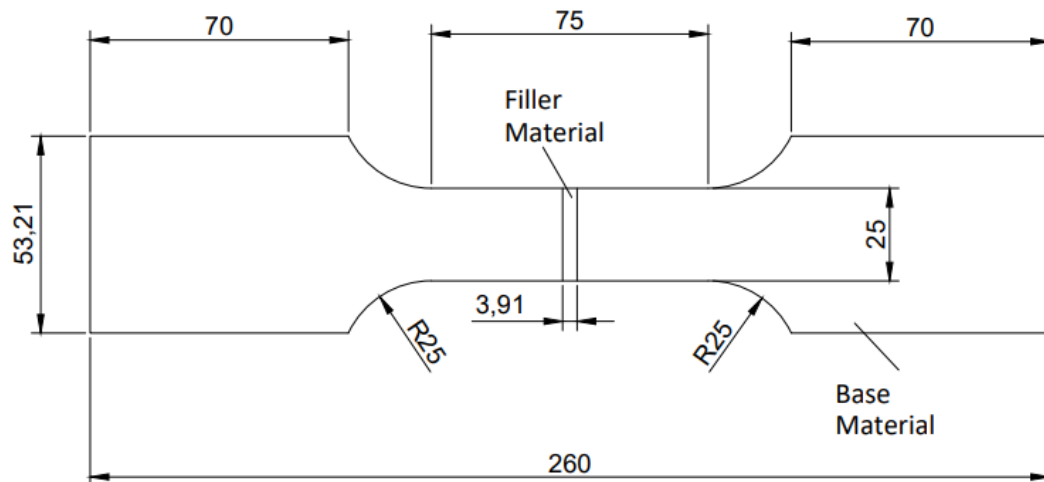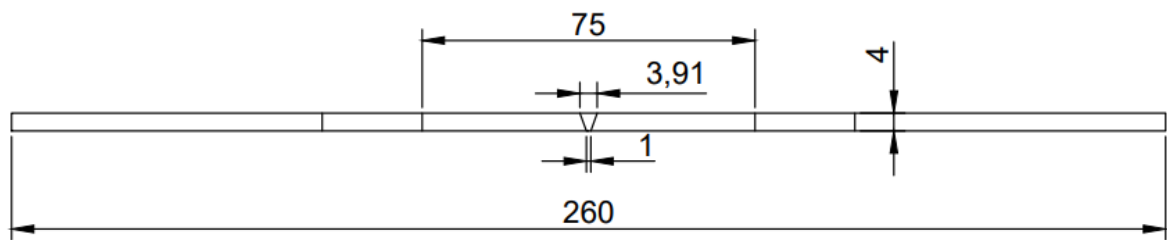Figure 3. The first drawing of the top view of the specimen

Figure 4. The first drawing of the side view of the specimen

An important aspect that requires modification in initial drawings is the inclusion of the data received after welding has been completed. Figure 5 provides a visual representation of the measurements obtained from HAZ after specimen was welded. To streamline the subsequent work and ensure simplicity, it has been decided to focus solely on the left side of the image as representative HAZ. Based on the data provided in the figure, the following input data for model is determined:

- WM bottom width: 19,684 – 8,025 - 8,745 = 2,914mm
- WM top width: 19,684 - 7,322 - 7,887 = 4,475mm
- HAZ top width: 7,322 – 6,207 = 1,115mm
- HAZ bottom width: 8,025 – 6,207 = 1,818mm

Figure 5. Cross section of the specimen after welding
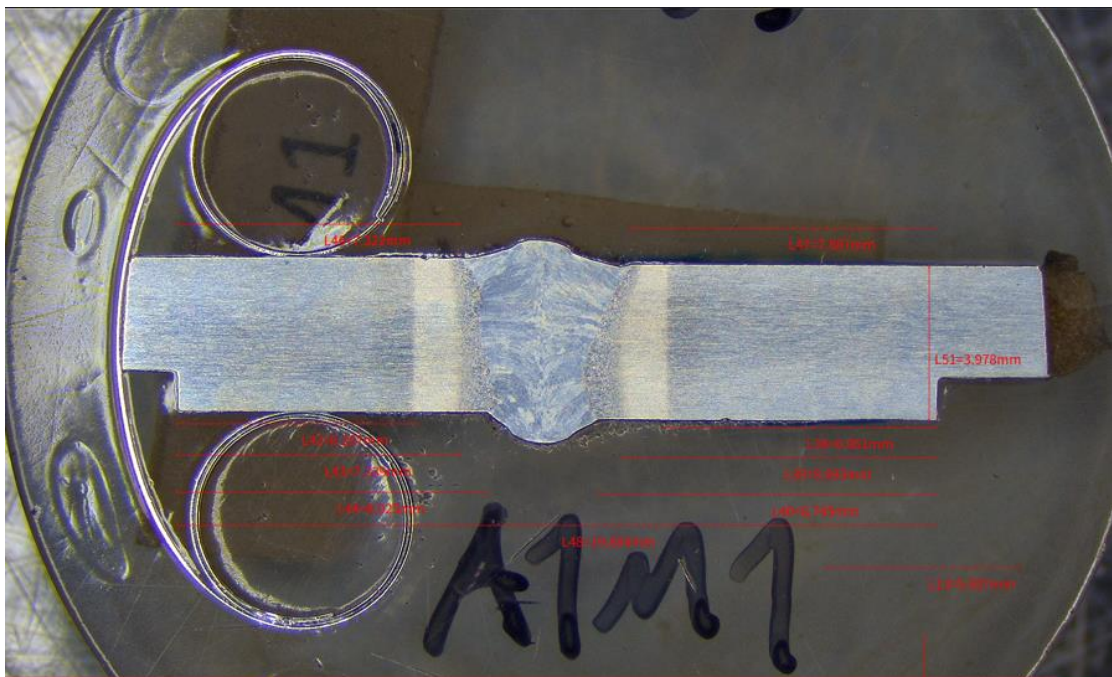
4.2 Experimental tensile tests

A Zwick/Roell Z250 tensile testing machine equipped with an extension meter 10-100mm and GOM ARAMIS 5M system was used to conduct standard quasi-static tensile tests. The tests were conducted in accordance with DIN EN ISO 6892-1 testing standard, and the tensile test samples were prepared following the EN ISO 15614 _1:2017 standard. The specimens had an initial gauge length of 50 mm and thickness of 4 mm.

The testing setup is composed of a test frame with various components, including testing software Test Expert 3, crossheads, clamping jaws, load cell, and extension meters. The tensile test is executed by securing the specimen to the pulling device with clamping jaws at the top and bottom crosshead. The dimensions of the specimen, such as thickness, width, total length, and gauge length, are recorded before the test, and all measured data are saved in the software program. The required testing parameters are then chosen on the control computer. Following this, a command is given through the software, and the device starts applying a gradually increasing tensile load to the specimen. This load is increased until the specimen breaks as it is shown in Figure 6.

Figure 6 The welding specimen after the fracture in the tensile test
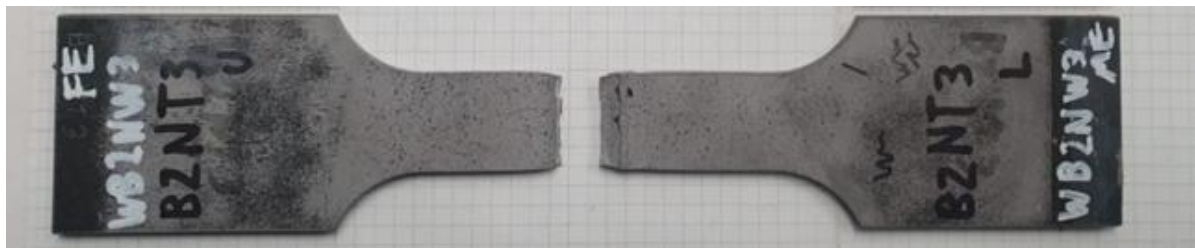
4.3   Key parameters in Finite Element Analysis

This subchapter offers a thorough overview of crucial parameters in Abaqus software, integral to model creation in this research. It delves into essential modules such as materials, sections, steps, also outlining applicable meshing techniques for the model.

4.3.1   Materials

In Abaqus, a material definition serves as a comprehensive specification encompassing all relevant property data associated with a particular material. The definition entails the inclusion of material behaviors and the provision of property data within each material behavior such as mass density, failure pattern, elastic, and plastic behavior. To facilitate this process, the material editor within Abaqus enables users to input all the necessary information that characterizes each material. (Simulia, ABAQUS/CAE User's Manual (v6.6) 12.2.1 Defining materials, n.d.) Each created material is assigned a unique name and remains independent of any specific section. Consequently, a single material can be referenced in multiple sections as needed. When assigning a section to a region of a part in Abaqus/CAE, the properties of the material associated with that section are automatically applied to the corresponding region. This approach allows for flexibility and efficiency in managing materials within Abaqus simulation. By defining materials separately and assigning them to relevant sections, users can accurately model and analyze the mechanical behavior of different regions within a part while maintaining consistency in material properties.

4.3.2   Sections

In Abaqus, a section is utilized to define the cross-sectional properties of a part or element in a finite element analysis. The primary objective of defining a section is to furnish Abaqus with the necessary information to calculate the behavior of a part or element when subjected to loads. A section comprises pertinent information about the properties of a part or a specific region within a part. The required information in a section definition varies based on the type of region under consideration. For instance, deformable wires, shells, or two-dimensional solids necessitate a section that encompasses details about their cross-sectional geometry. Similarly, a rigid region requires a section that describes its mass properties. Most sections are associated with a material name. (Simulia, ABAQUS/CAE User's Manual (v6.6) 12.2.3 Defining sections, n.d.) When assigning a section to a part, ABAQUS/CAE automatically applies the same section to each instance of that part. Consequently, the elements generated

during meshing will inherit the properties specified in the assigned section. Sections are named and created independently of any specific region, part, or assembly. It is possible to assign a single section to multiple regions as required. The property module in Abaqus facilitates the creation of solid sections, shell sections, beam sections, and other types of sections, providing a versatile approach to defining the properties of different parts or regions within a model.

4.3.3 Steps

The Step module in Abaqus offers various functionalities for performing tasks in the analysis process. It allows you to create analysis steps, define the sequence of changes in loading and boundary conditions, interactions between model parts, and additions or removals of parts. Steps provide flexibility in modelling dynamic scenarios and allow for modifications in analysis procedures, data output, and controls. You can also use steps for linear perturbation analysis and modify the analysis procedure of existing steps. (Simulia, ABAQUS/CAE User's Manual (v6.6) 14.1 Understanding the role of the Step module, n.d.) Additionally, the Step module enables you to specify output requests for extracting relevant data during the analysis. Output requests define the variables to be obtained, the regions from which the data will be extracted, and the frequency of recording. For example, you can request output of the displacement field of the entire model at the end of a step and track the history of reaction forces at specific points.

4.3.4 Mesh

The mesh module in Abaqus/CAE enables the generation of meshes on parts and assemblies, providing various levels of automation and control to meet the analysis requirements. Like the process of creating parts and assemblies, mesh attributes, such as seeds, mesh techniques and element types, are assigned in a feature-based manner. This allows for the modification of parameters defining the model, with automatic regeneration of the specified mesh attributes within the Mesh module (Simulia, ABAQUS/CAE User's Manual (v6.6) 17.1 Understanding the role of the Mesh module, n.d.).

Key features of the Mesh module include:

- Mesh Density Control: Tools are available to prescribe mesh density at both local and global levels, allowing for refined or coarse meshes based on specific regions or overall requirements.

- Visualization of Meshing Technique: The model coloring functionality visually indicates the assigned meshing technique for each region, aiding in understanding the meshing approach employed.

- Mesh Controls: A variety of mesh controls are provided, including options for element shape, meshing technique, meshing algorithm, and adaptive remeshing rules, offering flexibility in defining the mesh characteristics.

- Element Type Assignment: A tool allows for assigning ABAQUS/Standard and Abaqus/Explicit element types to mesh elements belonging to either a created model or an orphan mesh.

- Mesh Quality Verification: Tools are available to verify the quality of the generated mesh, ensuring optimal element shapes and mesh integrity.

4.4 Utilization of experimental data for the input of material model

The following subchapter explains the process of handling data derived from physical experiments, presenting fundamental formulas for converting this data into the input format of the finite element model. However, since simplified methods were used to estimate the stress-strain values, the data used in this research may not be very accurate and was not validated. Emphasis was put on the simulation process and its verification.

4.4.1 The plastic behavior

In Abaqus, like in majority of finite element analysis software, it is essential to input stress-strain data as true stress and true strain information. This involves correlating the material's present deformed state with the historical data from previously executed states, rather than relying on the initial undeformed states. (Mavrodontis, 2017). The true tensile stress and true tensile strain can be converted from engineering values using analytical equations 1 and 2.

Equation 1. True tensile stress

$$\sigma_{true} = \sigma_{eng} \times (1 + \varepsilon_{eng})$$

Equation 2. True tensile strain

$$\varepsilon_{true} = \ln\left(1 + \varepsilon_{eng}\right)$$

The stress-strain curves depicted in Figure 7 within this research thesis are true stress-strain curves calculated using analytical equations 1 and 2 in accordance with the ISO 10275:2020 standard. The curves reflect the experimental data obtained from the tensile tests for all three material types where grey color represents WM, orange represents HAZ, and blue represents BM. They show the true relation between stress and strain until the fracture of the materials, representing the maximum tension stresses that the specimen can withstand.

Figure 7. The True Stress-Strain curves of all three material zones
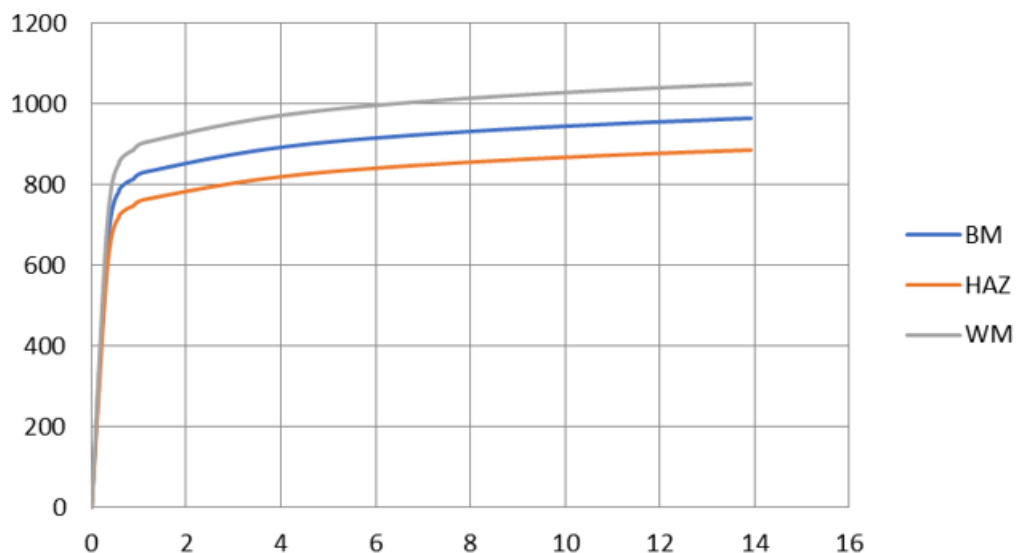
As shown in Figure 8, it is important to note that these equations are valid only until the UTS point. Within the plastic region (region in which even after load removal some permanent deformations shall remain) two sub-regions are distinguished, the work hardening region and the necking region. These two regions are separated by UTS point. In the necking subregion, the material experiences strain localization and a significant decrease in stress, leading to a reduction in the cross-sectional area of the specimen. (Mavrodontis, 2017)

Figure 8. The example representation of conversion validity (Mavrodontis, 2017).
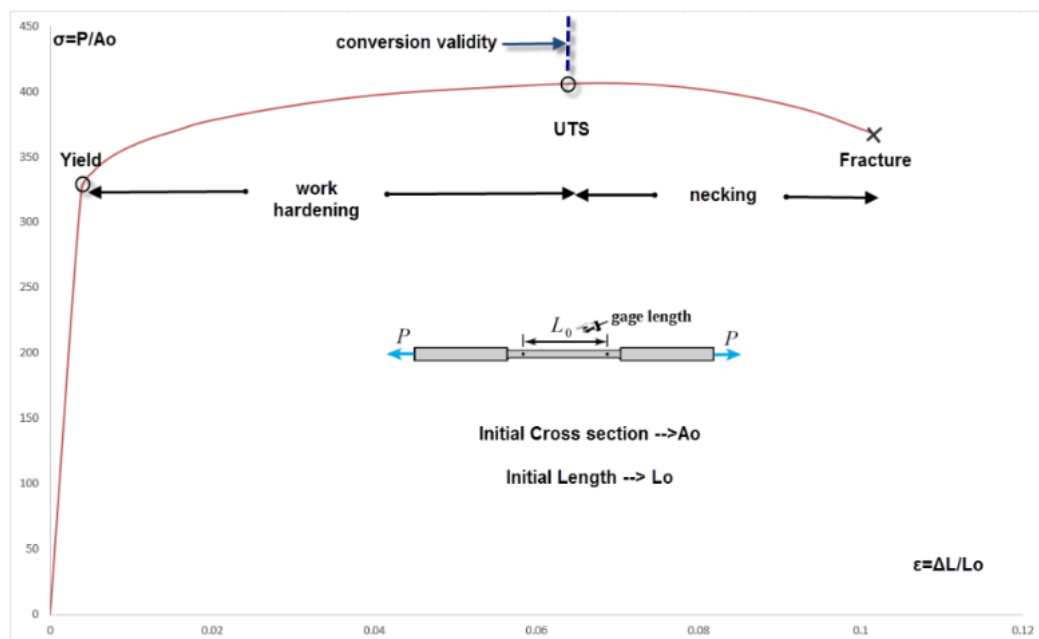
To include the plasticity within Abaqus, the stress-strain points past yield, must be input in the form of true stress and logarithmic (effective) plastic strain (Mavrodontis, 2017). The logarithmic plastic strain required by Abaqus can be calculated with the equation 3.

Equation 3. Logarithmic plastic strain

$$\varepsilon_{pl} = \varepsilon_{true} - \sigma_{true} \div E$$

To implement plasticity in Abaqus using the provided stress-strain data, it is crucial to ensure that the first data point corresponds to the yield point. Specifically, the yield stress should be associated with a logarithmic plastic strain value of 0. Figure 9 depicts the effective stress-strain curves after applying the equation where the grey color represents WM, the blue color represents BM, and the orange color represents HAZ.

Figure 9. The Effective Stress-Strain curves
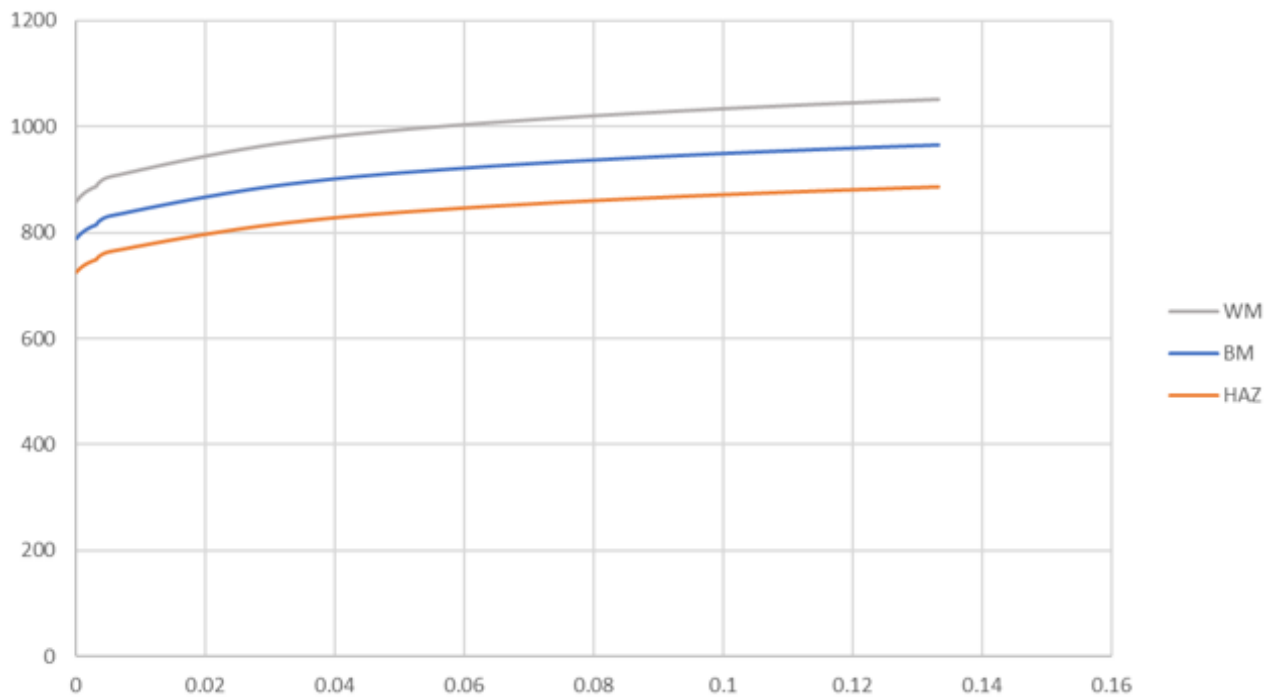
Table 3 provides the columns with input values for the plastic region of the model in Abaqus respectively from left to the right for HAZ, BM, and WM.

Table 3. The input values for plastic region

σ_{true}	ε_{pl}	σ_{true}	ε_{pl}	σ_{true}	ε_{pl}
724.600422	0	788.9740795	0	859.0349778	0
726.5410565	0.000135106	791.0871204	0.000135106	861.3356567	0.000135106
728.3688928	0.000273292	793.0773421	0.000273292	863.5026101	0.000273292
730.1527356	0.000418009	795.0196618	0.000418009	865.6174078	0.000418009
731.7886531	0.000562823	796.8009146	0.000562823	867.5568358	0.000562823
733.3452016	0.000710951	798.4957473	0.000710951	869.4021696	0.000710951
734.8205771	0.000864533	800.1021954	0.000864533	871.1512704	0.000864533
736.2345287	0.001022377	801.6417627	0.001022377	872.8275513	0.001022377
737.5300771	0.001176982	803.0524079	0.001176982	874.3634617	0.001176982
738.7915351	0.001337633	804.4259341	0.001337633	875.8589571	0.001337633
739.9881196	0.001501351	805.7288234	0.001501351	877.2775429	0.001501351
741.1814391	0.001678483	807.0281577	0.001678483	878.6922581	0.001678483
742.2460046	0.001846784	808.1872995	0.001846784	879.9543317	0.001846784
743.2617521	0.002016959	809.2932862	0.002016959	881.15853	0.002016959
744.2206225	0.002185797	810.3373429	0.002185797	882.2952989	0.002185797
745.1534935	0.002359361	811.3530903	0.002359361	883.4012447	0.002359361
746.0178245	0.002533371	812.2942086	0.002533371	884.4259344	0.002533371
747.3942841	0.002826291	813.7929532	0.002826291	886.0577675	0.002826291
747.7261954	0.002902329	814.1543516	0.002902329	886.4512581	0.002902329
748.4931714	0.003081115	814.9894659	0.003081115	887.3605305	0.003081115
752.9803629	0.003330056	819.8753004	0.003330056	892.6802271	0.003330056
761.6912968	0.004565292	829.3601157	0.004565292	903.0072939	0.004565292
768.5146937	0.007282959	836.7897046	0.007282959	911.0966304	0.007282959
777.6266505	0.011206795	846.7111695	0.011206795	921.8991214	0.011206795
789.7232382	0.01665531	859.8824208	0.01665531	936.2399797	0.01665531
803.2014479	0.02336023	874.5580375	0.02336023	952.2187912	0.02336023
815.9639069	0.030840153	888.4543161	0.030840153	967.3490594	0.030840153
828.7373184	0.04051516	902.3625202	0.04051516	982.4923119	0.04051516
838.5842019	0.05028452	913.084203	0.05028452	994.1660802	0.05028452
847.9983792	0.061663084	923.3347378	0.061663084	1005.326863	0.061663084
856.9149641	0.074110591	933.043474	0.074110591	1015.897734	0.074110591
864.9317246	0.087110933	941.7724453	0.087110933	1025.401838	0.087110933
872.2690845	0.100724371	949.7616577	0.100724371	1034.100493	0.100724371
878.6840703	0.1141379	956.7465523	0.1141379	1041.705646	0.1141379
884.5394212	0.127749374	963.1220938	0.127749374	1048.647336	0.127749374
886.7939637	0.133366568	965.5769303	0.133366568	1051.320162	0.133366568

4.4.2   Fracture of the material

Figure 10 illustrates the characteristic stress-strain behavior of a material undergoing damage. Abaqus offers a range of standard options for damage initiation in ductile metals, each associated with distinct material failure criteria related to metal fracture. In this thesis, the focus is on ductile damage evolution, involving the calculation of fracture energy.

Figure 10. Stress-Strain curve with progressive damage degradation (Wagner, 2021).
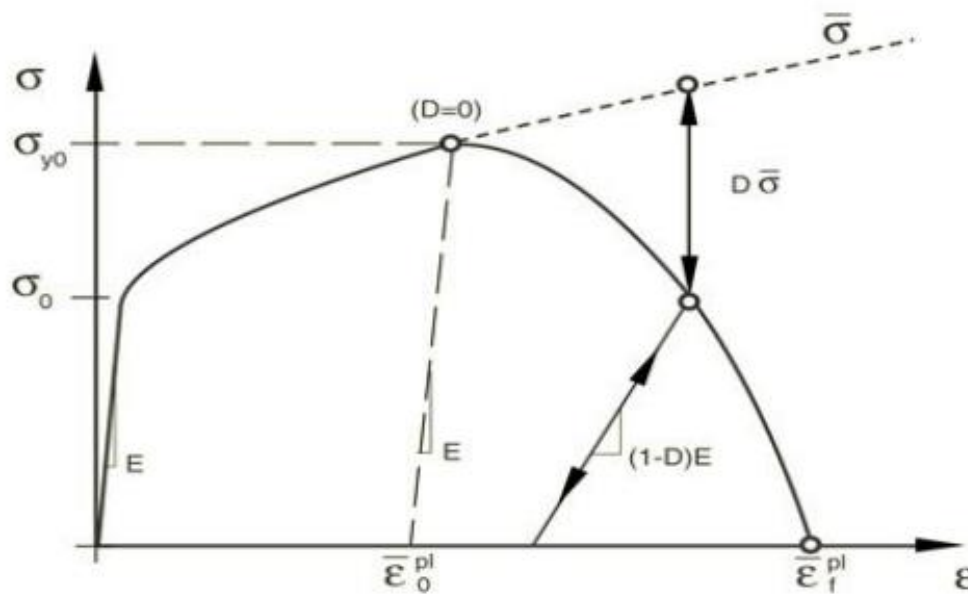
Fracture energy evolution defines damage in terms of the energy required for failure after the initiation of the damage (Wagner, 2021). The fracture energy can be calculated using the equation 4.

Equation 4. Fracture energy

$$G_f = \int_{\varepsilon_0^{pl}}^{\varepsilon_f^{pl}} L\sigma_y d\varepsilon^{pl}$$

Characteristic element length is primarily used by Abaqus for the regularization of models displaying strain softening or as a parameter passed to user subroutines invoked at material points. By default, Abaqus calculates the characteristic element length employing a geometric mean-based definition. (Wagner, 2021)

For a simple C3D8 element, the characteristic element length can be calculated using equation 5.

Equation 5. The characteristic length

$$L = V \div A$$

4.5 Finite element modeling of tensile tests

The following subchapter explains how to start modelling the specimen in Abaqus using the values received after the conversion of the initial experimental data. It provides the explanation of the key tools used for modelling.

4.5.1 Geometry modelling

The initial step to create a solid model is to collect accurate measurements and dimensions of the steel specimen. Figures 3 and 4 depict various perspectives and drawings of the tensile specimen. This way these figures present the necessary measurements for constructing the solid model's geometry. The procedure for constructing the solid model's geometry can be divided into four main steps:

- Initial geometry creation
- Creation of material models and section assignment
- Element type confirmation and assignment
- Mesh generation and confirmation

The model created in this study is a solid model type. The initial geometry creation of the part starts by drawing the geometry in the Abaqus sketcher. Figure 11 shows the initial geometry of the specimen made in the Abaqus sketcher. The Abaqus sketcher allows the user to pick geometry-based tools on the left-side menu and sketch in the main window as per any CAD utility (Austin, 2016).

Figure 11. The initial geometry of the specimen
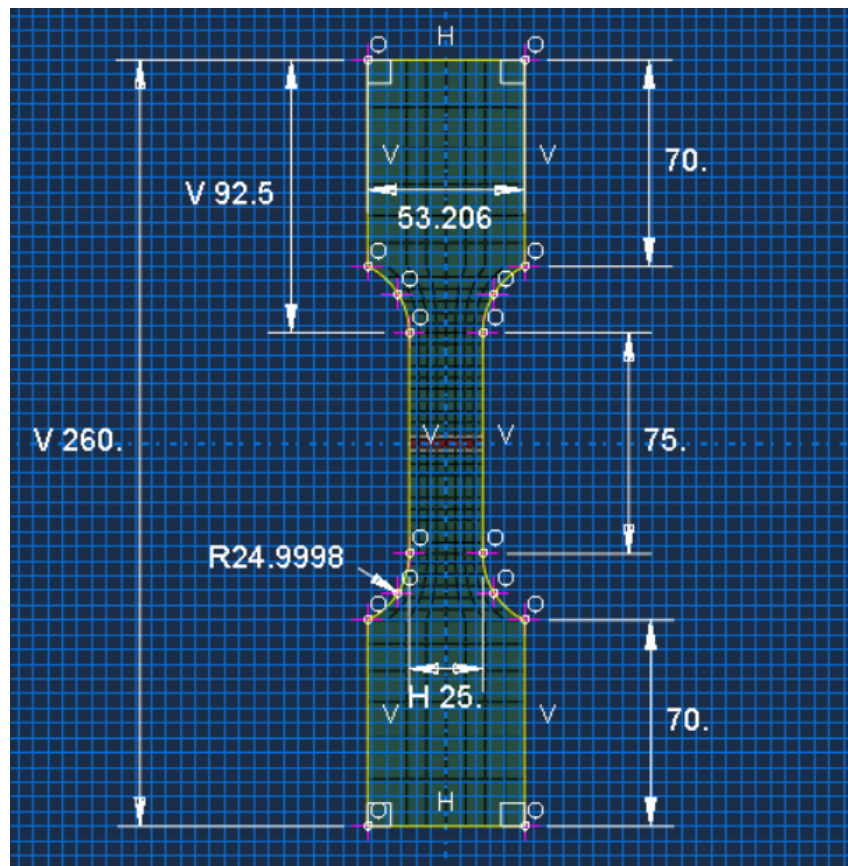
Once the geometry has been created the depth of the extrusion is determined to specify the thickness of the specimen which is 4mm in this case study.

Leveraging the capabilities of Abaqus, a three-dimensional solid geometry is constructed to accurately resemble the steel specimen. The length, width, and height dimensions of the specimen are defined within the software, and specific features such as fillets and surface irregularities are incorporated as required by the study. In the Part module you can use the Partition toolset to separate the element into additional regions. After you separate an element, you can use the Property module to assign various sections to the new regions. In this study case this toolset is used for separating the part into different cells. Figure 12 depicts different cells of the model such as crosshead, fillet, gauge, HAZ and WM. The values of layer thicknesses provided in Figure 4 were initial values that were then adjusted according to the data received after welding in Figure 5. The result of this adjustment is shown in the Figure 13.

Figure 12. The partitioned specimen
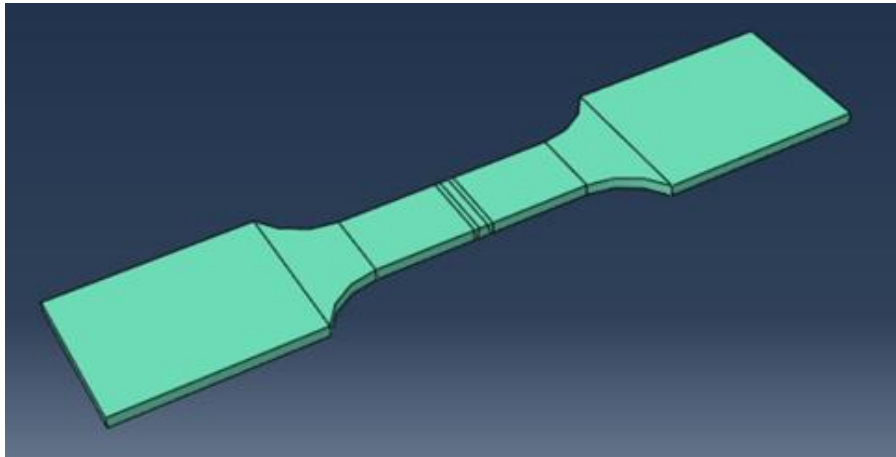
Figure 13. Cross-section of the specimen in the model after welding
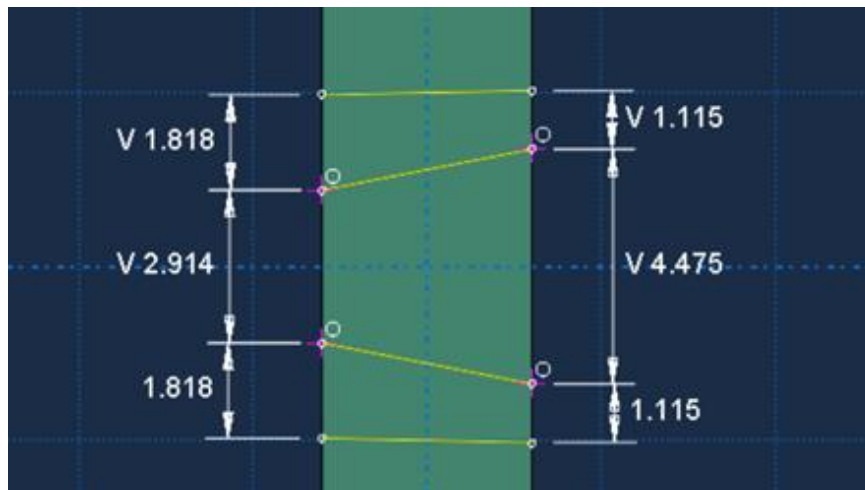
4.5.2 Material creation and section assignment

To establish precise material behavior within the context of the tensile specimen, this study employs three distinct material models, specifically designed to represent HAZ, BM, WM regions. It is important to note that Abaqus lacks inherent dimensional units; therefore, it is essential to ensure that all input parameters are consistently expressed in compatible units. For example, for the purpose of this research, dimensional values are denominated in millimeters (mm), while applied loads are expressed in Newtons (N). The exact input values for all three material models can be found in Appendix number 2. Figure 14 depicts the material model menu to apply the material behaviors. Each material model employed in this thesis encompasses four distinct material behaviors:

- Mass Density defines the materials' resistance to deformation and its ability to transmit and distribute forces within a given volume.
- Elastic behavior describes a material response to applied loads in reversible manner. It is defined through material properties such as Young's Modulus (E) and Poisson's Ratio (v).
- Plastic behavior pertains to irreversible deformation that occurs in a material beyond its elastic limit. It is defined through true stress (σ_{true}) and corresponding effective plastic strain (ε_{pl}).
- Ductile Damage behavior delineates the failure mechanism of the specimen. It is characterized by factors such as fracture strain (ε_0^{pl}), stress triaxiality (η), strain rate (ϵ), and the fracture energy (G_f)

Figure 14. The material model menu
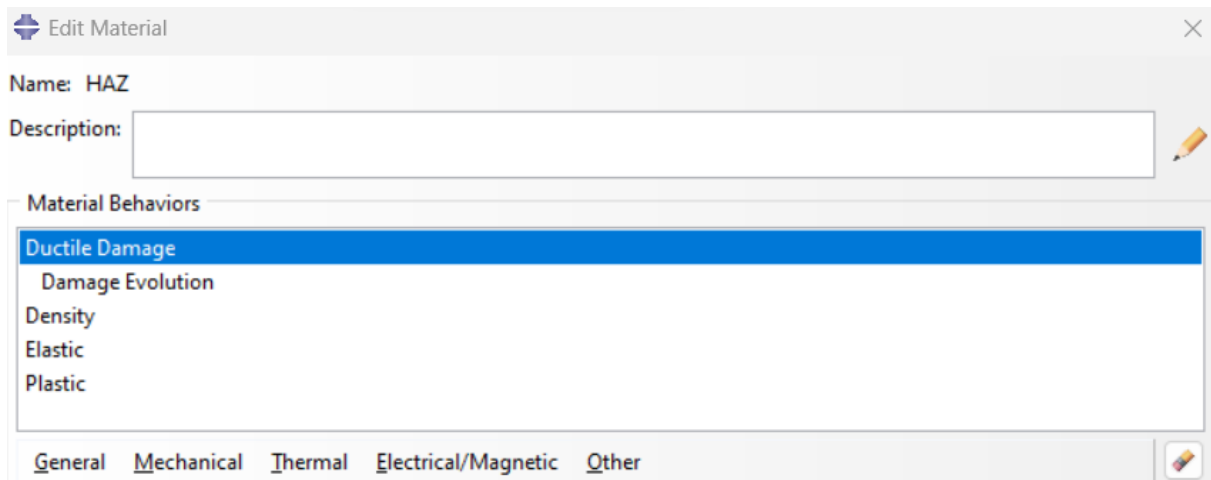
When material models are established, the subsequent step involves the creation of corresponding sections. These sections are essential for defining the material properties and behavior within the selected section. Once the sections are defined, they can be assigned to specific regions of the specimen model. Figure 15 visually represents the assigned sections in the model, where green corresponds to BM, white corresponds to HAZ, and red corresponds to WM.

Figure 15. Sections of the model
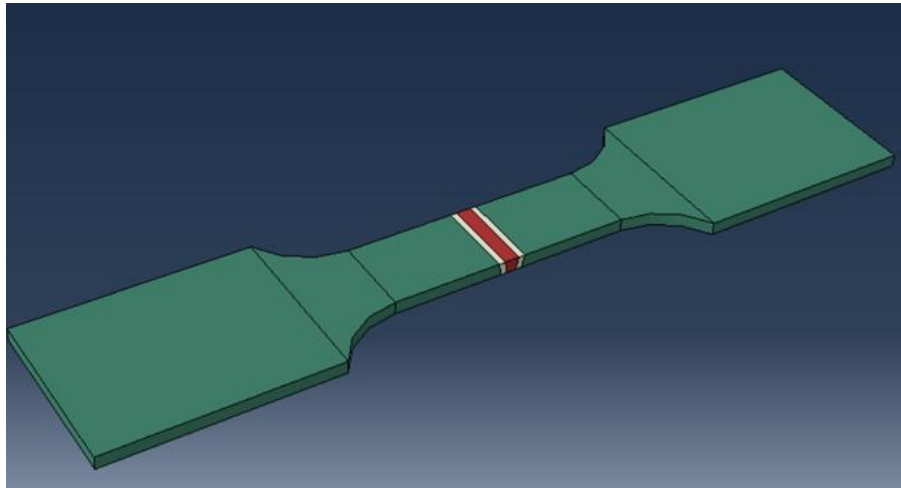
4.5.3   Mesh creation and Element type assignment

Mesh size is a common challenge in FEM. Skotny (2017) states that using bigger elements can yield inaccurate results, while smaller elements can significantly prolong computational time. Therefore, it was decided to perform the preliminary simulations with a coarse mesh to get the basic idea if the simulation is going in the right direction, as it saves a significant amount of computational time. Meanwhile, the results will be received from the model with a finer mesh.

According to Skotny (2017) the smaller meshes generally provide more accurate results. Therefore, it was decided to apply finer mesh in the critical area where the highest stress occurs, while the rest of the model has a coarse mesh. Figure 16 represents the coarse mesh with an average size of 2mm in the entire model, meanwhile, Figure 17 depicts the finer mesh in the area of the highest stress.

Figure 16. The coarse mesh
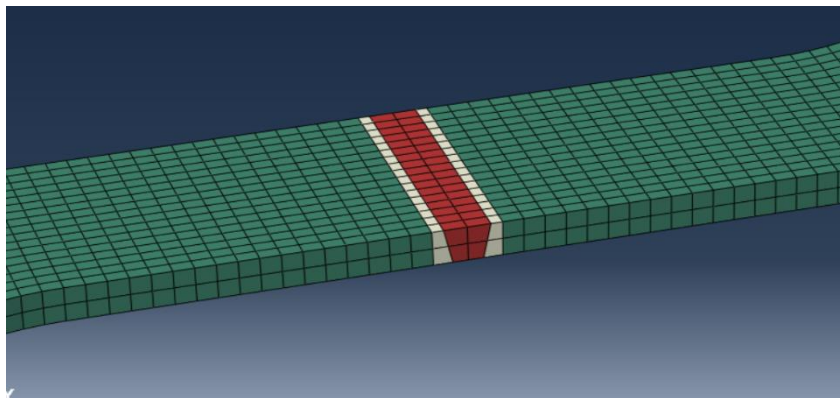
Figure 17. The fine mesh
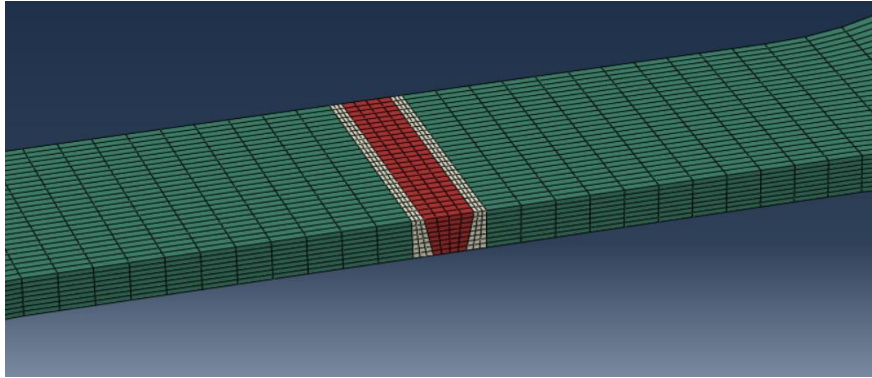
4.5.4 Step Module

During the modeling process, there exist other ways to optimize computational efficiency by judiciously employing step module features. For instance, one can reduce the simulation time interval from the standard 1 second to 0.1 second while simultaneously implementing mass scaling techniques, as it is shown in Figure 18. It is noteworthy that the mass scaling factor, although instrumental in expediting simulation runs, is not applied when retrieving final simulation results. Instead, it is judiciously employed during preliminary trial simulations to assess the model's behavior and ensure the efficiency of the simulation process. By leveraging these techniques, researchers can significantly enhance the computational efficiency of the Abaqus simulations while maintaining a rigorous and iterative approach to model validation.

Figure 18. The mass scaling tab of the step module
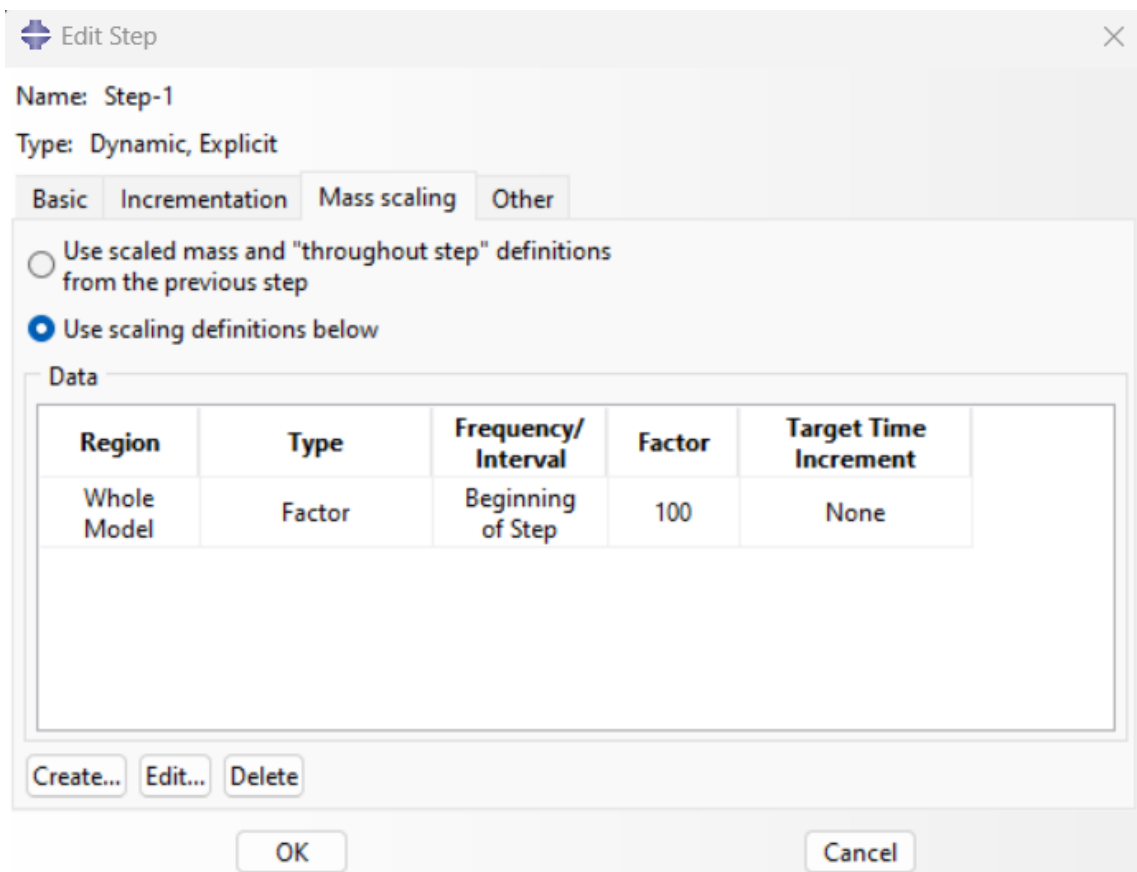
4.5.5 Constraint and Boundary Conditions

To perform the tensile test, the reference point is created with a small offset from the surface of the crosshead. Subsequently, a coupling constraint is assigned to this reference point and to the crosshead of the specimen, as it is shown in Figure 19. This step serves to immobilize the crosshead cell within the model, effectively anchoring it to the reference point. Consequently, the controlled application of force to the reference point initiates the stretching of the specimen, thereby enabling the simulation of tensile deformation.

Figure 19. The coupling constraint of the crosshead
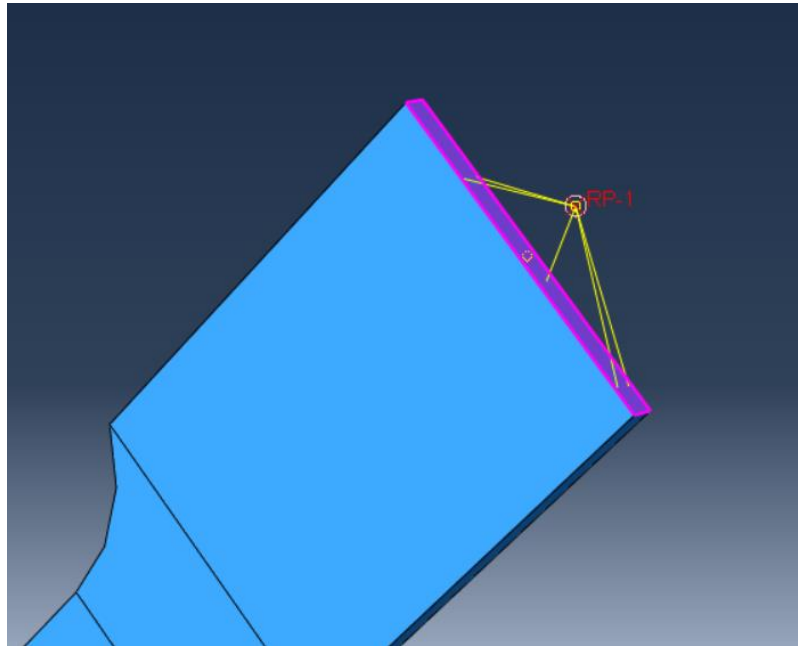
To ensure the static stability of the lower crosshead during the tensile test, a fixed boundary condition is applied, as shown in Figure 20. This boundary condition ensures the immobility of the lower crosshead. To enact the force upon the specimen, a displacement boundary condition is applied to the previously established reference point, as shown in Figure 21.

Figure 20. The fixed boundary condition of lower crosshead
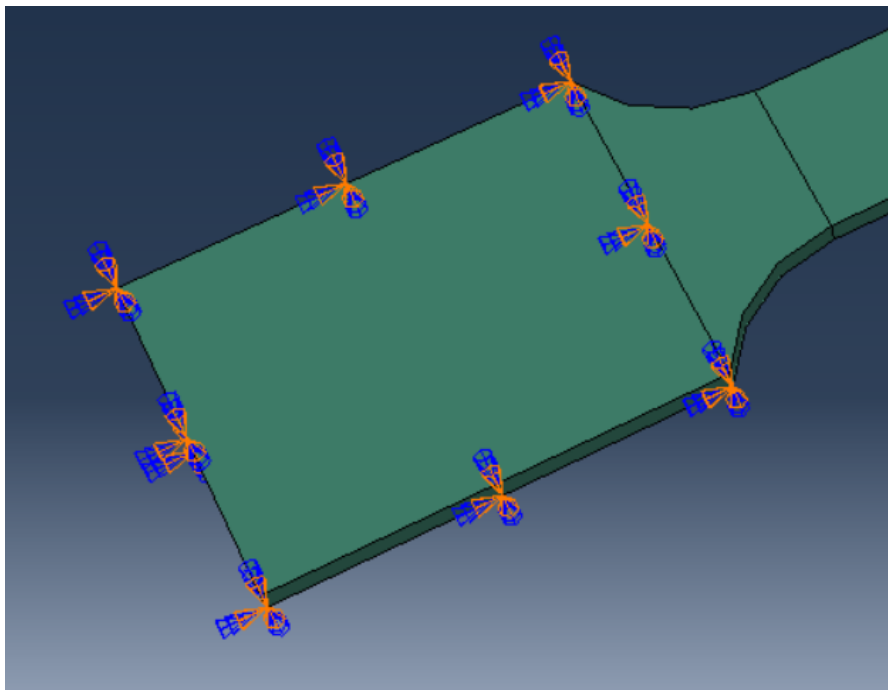
Figure 21. The displacement boundary condition of the upper crosshead
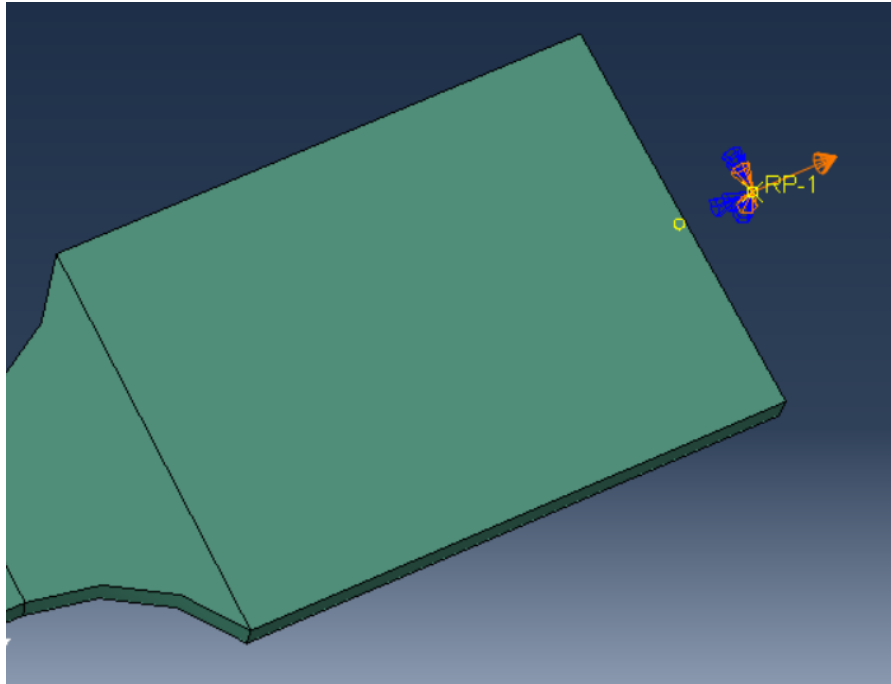
5   Results from FEA and comparison to the experimental results

This chapter presents the results of the tensile simulation from the finite element model created in this thesis and compares them to the experimental results received in the laboratory to evaluate the accuracy of the simulation. The simulation results contain:

- Failure of the model
- Engineering Stress-strain curves of three material zones
- Force-displacement curve of the model

5.1   Failure of the model

Figures 22 and 23 illustrate the failure pattern observed in the simulation model, mirroring the laboratory specimen's failure behavior, as evidenced in Figure 6. Notably, the fracture occurs within the stretched heat-affected zone, demonstrating a consistent and accurate replication of the laboratory specimen's failure characteristics.

Figure 22. The front view of the model failure
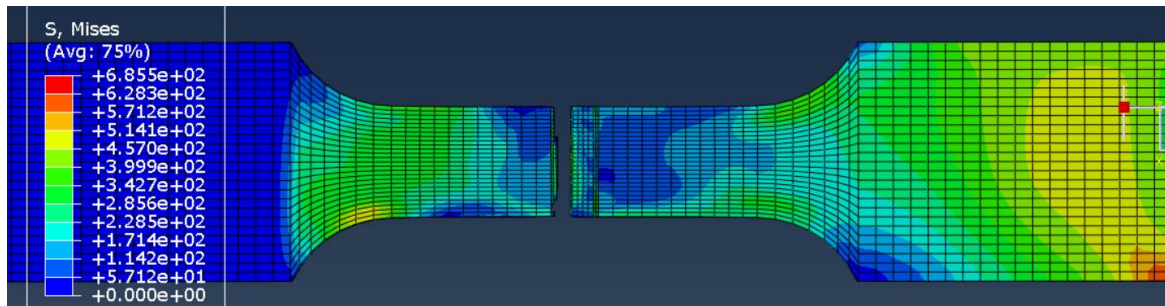
Figure 23. The side view of the model failure
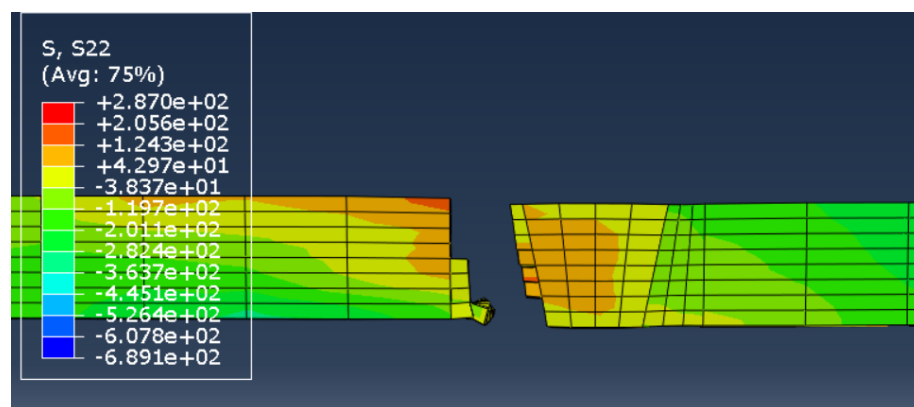
5.2 Stress-strain curves

Figures 24, 25 and 26 depict the engineering stress-strain graphs, with the orange line representing results obtained from the simulation, and the blue line representing experiment data. Comparing these graphs reveals that the transitions from elastic to plastic regions are notably similar, thereby signifying the robustness of the finite element model in replicating the material's behavior under tensile loading conditions. It is pertinent to acknowledge that post the ultimate point, dissimilarities in the curves become apparent. Nonetheless, it must be emphasized that the principle of this thesis does not entail achieving an exact replication of post-ultimate behavior.

Considering this, the observed similarities and controlled deviations post-ultimate point are well within the intended scope of this thesis. Consequently, the outcomes presented herein are deemed satisfactory for the objectives outlined in this research, affirming the utility of the finite element model in advancing our comprehension of tensile material behavior.

Figure 24. Engineering Stress-strain curves of HAZ
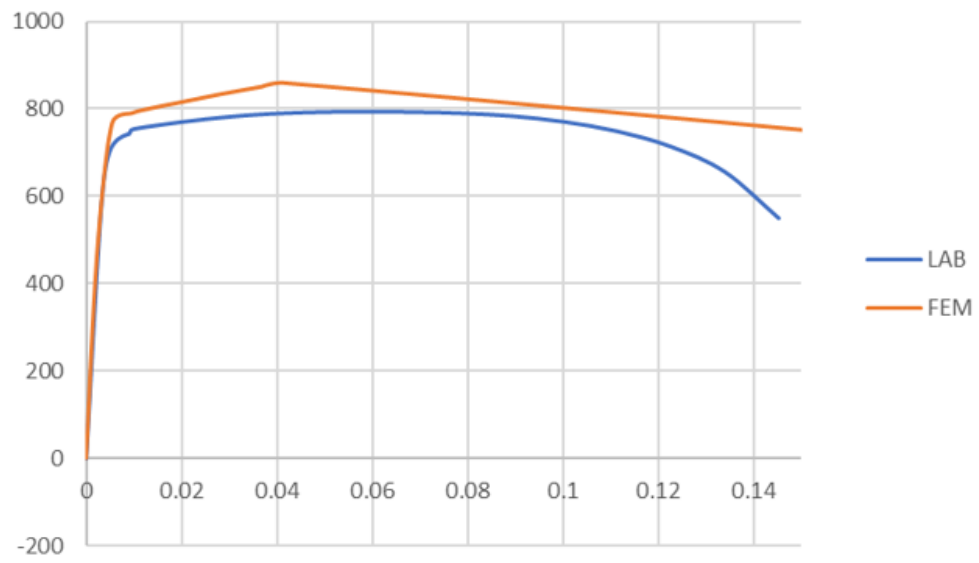
Figure 25. Engineering Stress-strain curves of BM
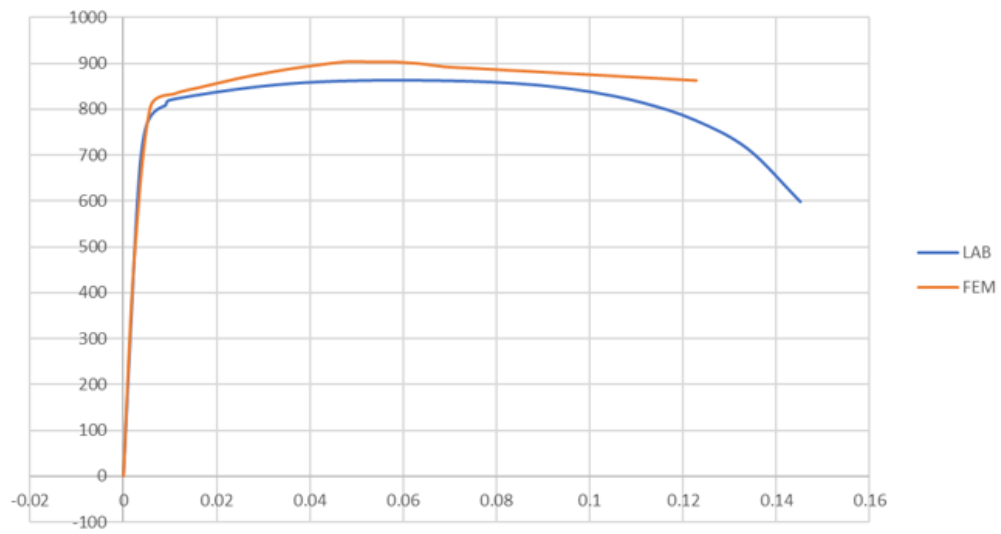
Figure 26. Engineering Stress-strain curves of WM
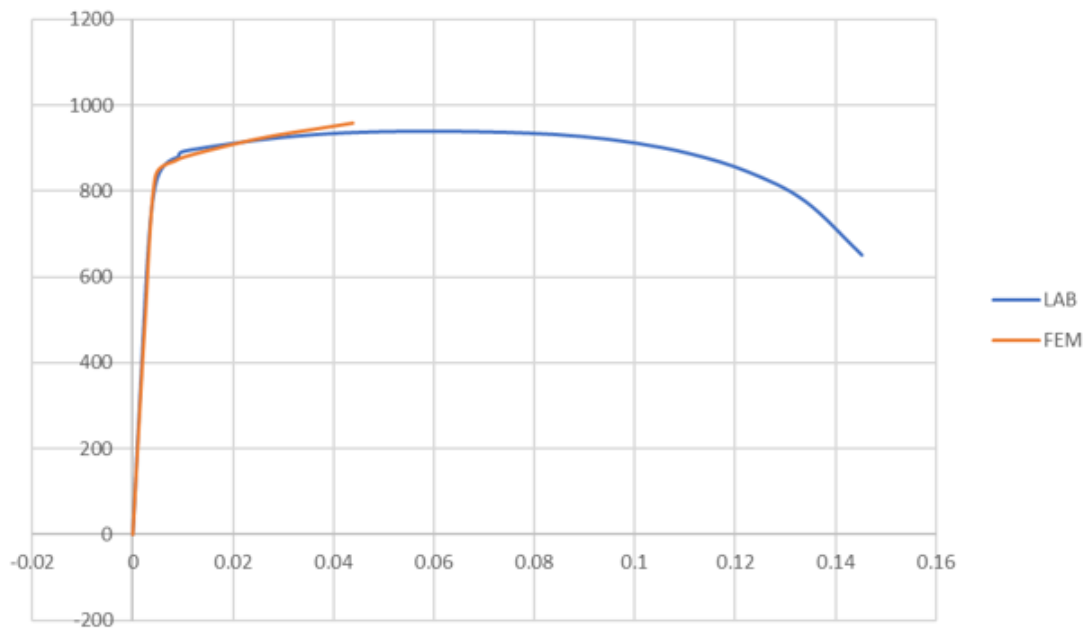
5.3 Force-displacement curve

Figure 27 presents the force-displacement graph of the model generated from the simulation, alongside the corresponding maximum force attained during the simulation process. It is obligatory to note that the laboratory test yielded a maximum force (Fm) value at 87.3 kN, meanwhile the simulation reached the value of 86.7 kN. Therefore, this congruence in results is considered both noteworthy and satisfactory for the purposes of this thesis.

Figure 27. The Force-Displacement curve of the model
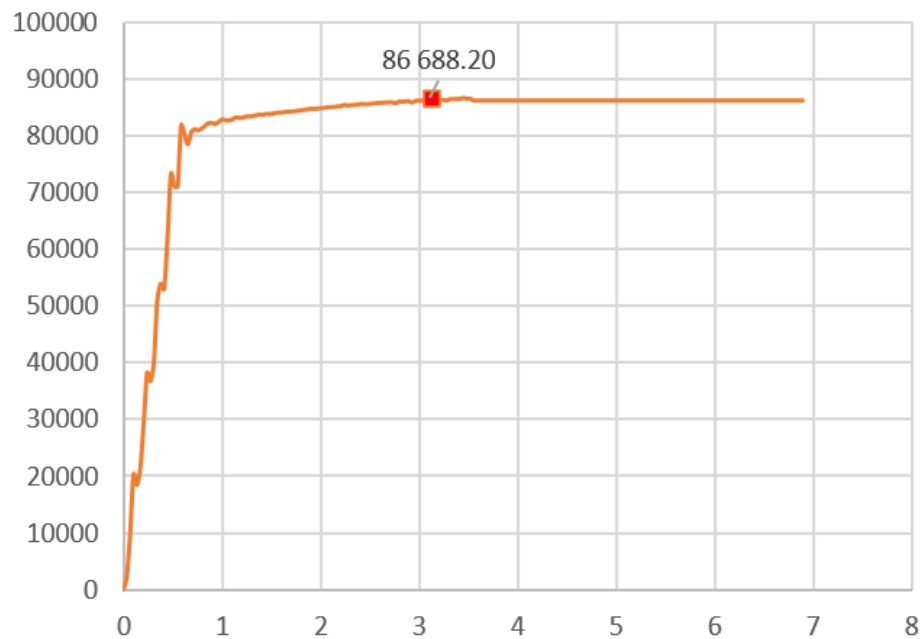
6   Analysis and discussion

Comparing results showed that the fracture in the simulation progresses according to the real test, showcasing the consistent fracture characteristics within the heat-affected zone. The stress-strain curves exhibit notable similarities, particularly in the elastic-to-plastic transitions. Moreover, the maximum force of 86.7 kN achieved via simulation aligns closely with a laboratory result at 87.3 kN. Accordingly, the error in maximum force is less than one percent.

Throughout the course of work, the necessity for the model adjustments became apparent. While experimenting with the model, the computational time became a pivotal factor, prompting the application of mass scaling and a larger mesh size. This approach ensured a computational time of approximately 5 minutes for the simulation. Otherwise, the final and more accurate simulation took up to 10 hours to complete. Therefore, before starting the accurate simulation the certainty in input values had to be ensured by running quicker simulations.

The questions mentioned in the objective of the thesis are provided with conclusive answers, as the entire modeling process using Abaqus is explained and the relevant practical examples with required input data are provided. Moreover, the accuracy of the simulation is evaluated by comparing the simulation results to the experimental data.

7 Conclusion

The objective of this thesis is to determine the best ways to work with Abaqus and to provide instructions on using Abaqus for modeling HSS. The research process of this thesis involves the recreation of one tensile testing specimen of HSS with a yield strength of 700 MPa. This thesis aims to simulate the specimen's tensile experiment and receive stress-strain graphs for all three material models nearly identical to the graphs received from the laboratory, as well as a force-displacement curve that would resemble a similar pattern. To accomplish that, the thesis describes all material properties that are required as input data, provides the instructions for using main tools of Abaqus and shows how to convert data from the experiments into input data. To evaluate the accuracy of the simulation, the simulation results are compared to the experiment results and analyzed.

The results of the simulation analyzed in this thesis seem satisfactory, as the results of the simulation align closely with the results of the experiment. Moreover, this thesis shows the alternative ways of modeling to reduce the computational time of the simulation.

8 Suggestions for improvements and future research

This thesis is a part of the larger research project conducted in HAMK Tech, therefore it can be used as a more accessible starting point for future research in the field of finite element modeling of HSS. Even though the thesis provides the instruction on creation of finite element model, some aspects were neglected due to the limitations of this study. Hence, further study should focus more on the behavior of the material past the UTS point and failure pattern of the specimen. Moreover, the further study should consider the validation and verification of the model which process is illustrated in Figure 28. This figure shows that the verification focuses on the mathematical aspects of FEA, determining if the solution that has been computed is accurate (McCaslin, 2021). On the other hand, validation is concerned with the accuracy of the model and looks at how well it captures the physical behavior of the real-world situation it is meant to simulate. Obbink-Huizer (2021) explains the advantages and disadvantages of implicit and explicit solvers, as well as the challenges related to each numerical solution such as incrementation algorithms, computational cost, time increment size and so on. Therefore, this might help in achieving more accurate results in the simulations. The proper validation of the finite element analysis can be achieved through the digital image correlation engine (DIC). For this reason, Lava, Jones, Wittevrongel, & Pierron (2020) investigate two full-field validation approaches in the journal article, exploring the challenges and solutions related to strain

formulations, coordinate systems, data locations, strain calculation algorithms, spatial resolutions, and data filtering for meaningful and quantitative FEA validation.

Figure 28. Illustration of the validation and verification process (Dunai, et al., 2023)
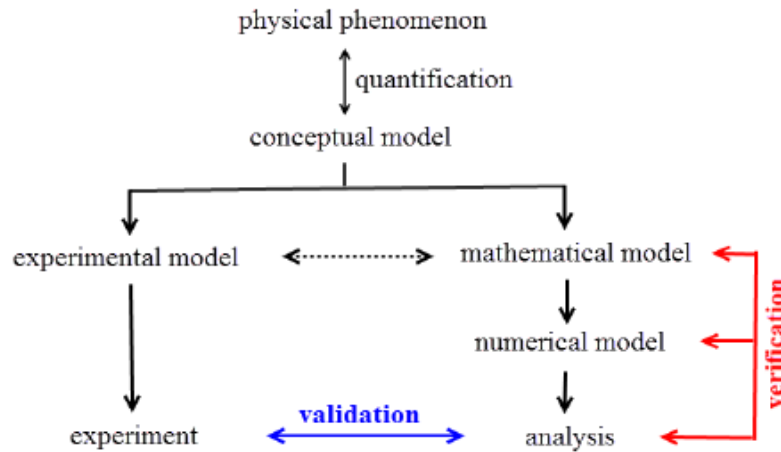
The new standard EN 1993-1-14 provides a systematic validation and verification on the process for comparing Finite Element Analysis results to experiments, emphasizing the importance of ensuring accuracy and proper implementation of numerical models. The concept of a standard design case allows for a one-time validation based on initial experience with similar models, streamlining subsequent model applications.

References

Austin, G. (2016, December 7). *Creating a new part in Abaqus/CAE*. Retrieved February 7, 2023, from Technia: https://www.technia.com/blog/creating-a-new-part-in-abaquscae/

Dunai, L., Kövesdi, B., Gardner, L., Al-Emrani, M., Casafont, M., Degée, H., . . . Walport, F. (2023). Design assisted by finite element analysis – Introduction to prEN 1993-1-14 and Technical Report. *ce/papers*.

ESAB. (2023, October 26). *OK Aristorod 89*. Retrieved from https://esab.com/ao/mea_en/products-solutions/product/filler-metals/mig-mag-wires-gmaw/low-alloy-wires/ok-aristorod-89/

Hajro, I. (2017). Mechanical Properties of Heat-Affected Zone of High-Strength Steel Welds.

Lava, P., Jones, E. M., Wittevrongel, L., & Pierron, F. (2020, April 20). Validation of finite-element models using full-field experimental data: Levelling finite-element analysis data through a digital image correlation engine. *Strain*.

Mavrodontis, N. (2017, October 8). *Converting Engineering Stress-strain to True Stress-strain in Abaqus.* Retrieved January 7, 2023, from https://simulation-blog.technia.com/simulation/converting-engineering-stress-strain-to-true-stress-strain-in-abaqus

McCaslin, S. (2021, February 4). *Validation and Verification in Finite Element Analysis (FEA)*. Retrieved from Control Automation: https://control.com/technical-articles/validation-and-verification-in-finite-element-analysis-fea/

Ngo, D. L. (2021). *Finite element simulation of heat affected zone of welded joint in high strength steel.* Bachelor's Thesis, Häme University of Applied Sciences. Retrieved from https://hamk.finna.fi/Record/theseus_hamk.10024_415875?sid=3481466995

Obbink-Huizer, C. (2021, July 26). *Implicit Vs Explicit Finite Element Analysis: When to Use Which?* Retrieved from Simulation: https://simulation-blog.technia.com/simulation/implicit-vs-explicit-finite-element-analysis

Peltonen, M. (2014). *Weldability of high-strength steels using conventional welding methods.* Master's Thesis, Aalto University. Retrieved from https://finna.fi/Record/aaltodoc.123456789_14537?sid=3481562785&imgid=1

Pham Nguyen, V. (2018). *Effect of heat input on the mechanical properties of butt-welded steel joints: Tensile and hardness test.* Bachelor's Thesis, Häme University of Applied Sciences. Retrieved from https://hamk.finna.fi/Record/theseus_hamk.10024_152688?sid=3480712867&imgid =1

Pirinen, M. (2013). *THE EFFECTS OF WELDING HEAT INPUT ON THE USABILITY OF HIGH STRENGTH STEELS IN WELDED STRUCTURES.* PhD Thesis, LUT University. Retrieved from https://finna.fi/Record/uef.9911331553705966?sid=3482035963

Rahman, M. M. (2022). *Heat affected zone stress-strain relationship in high strength steel welds.* Master's Thesis, LUT University. Retrieved from https://lutpub.lut.fi/handle/10024/163824

Sefcikova, K. (2015). Mechanical Properties of Heat Affected Zone of High Strength Steels. *IOP Conference Series: Materials Science and Engineering*, 15.

Simulia. (n.d.). *ABAQUS/CAE User's Manual (v6.6) 12.2.1 Defining materials*. (Simulia, Editor) Retrieved from https://classes.engineering.wustl.edu/2009/spring/mase5513/abaqus/docs/v6.6/boo ks/usi/default.htm

Simulia. (n.d.). *ABAQUS/CAE User's Manual (v6.6) 12.2.3 Defining sections*. Retrieved from https://classes.engineering.wustl.edu/2009/spring/mase5513/abaqus/docs/v6.6/boo ks/usi/default.htm

Simulia. (n.d.). *ABAQUS/CAE User's Manual (v6.6) 14.1 Understanding the role of the Step module*. Retrieved from https://classes.engineering.wustl.edu/2009/spring/mase5513/abaqus/docs/v6.6/boo ks/usi/default.htm

Simulia. (n.d.). *ABAQUS/CAE User's Manual (v6.6) 17.1 Understanding the role of the Mesh module*. Retrieved from https://classes.engineering.wustl.edu/2009/spring/mase5513/abaqus/docs/v6.6/boo ks/usi/default.htm

Simulia. (n.d.). *Getting Started with ABAQUS (v6.6). Finite Elements and Rigid Bodies. Finite Elements. Continuum Elements*. Retrieved from https://classes.engineering.wustl.edu/2009/spring/mase5513/abaqus/docs/v6.6/boo ks/gsa/default.htm

Skotny, Ł. (2017). *Correct mesh size - a quick guide!* Retrieved October 27, 2023, from
     Enterfea: https://enterfea.com/correct-mesh-size-quick-guide/

SSAB. (2023, October 26). *Strenx® 700MC Plus*. Retrieved from
     https://www.ssab.com/en/brands-and-products/strenx/product-offer/700/mc-plus

Wagner, R. (2021). *ABAQUS Tutorial: Damage for Ductile Metals - Material Model Explained -*
     Ductile Damage. ResearchGate. Retrieved from
     https://www.researchgate.net/publication/350124892_ABAQUS_Tutorial_Damage_f
     or_Ductile_Metals_-_Material_Model_Explained_-_Ductile_Damage

Appendix 1. Step by Step instruction

1. Go to **Part** Module and create the geometry of the specimen.
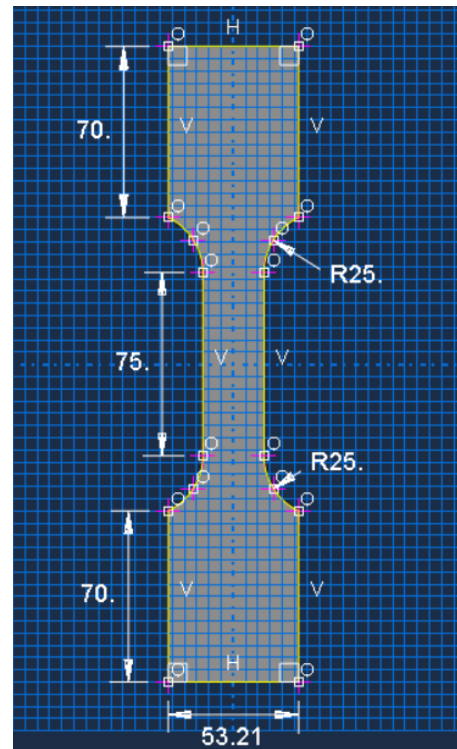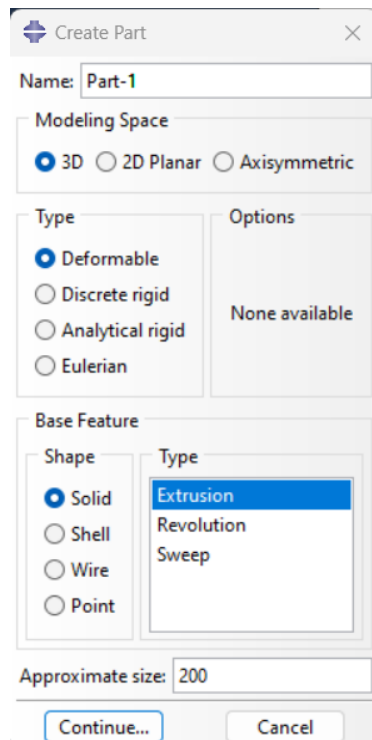
2. Use **Partition Face: Sketch** tool to separate the specimen part into separate zones. Green - Gripping section (BM), Middle section (BM), Gauge section (BM); white – HAZ; red - WM. Go to **Assembly** Module and Create **Instance** by choosing the created part and choosing **Dependent** type.
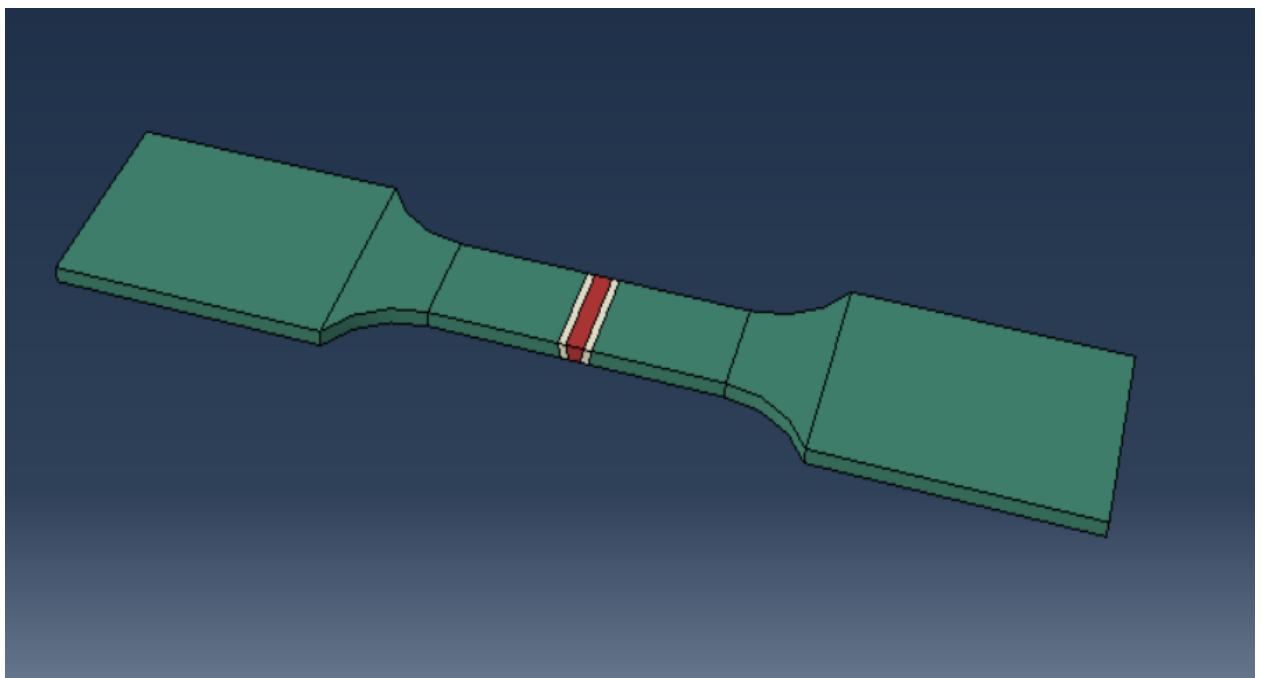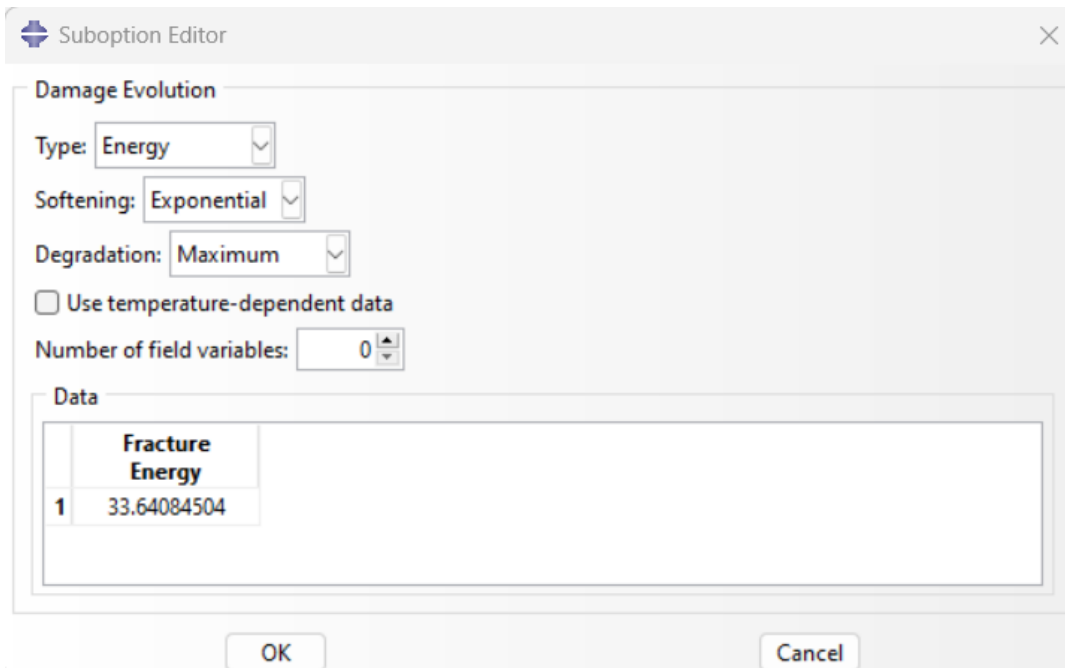
3. In the **Property** Module go to **Material Manager**. Create **material** models. In the following steps the procedure of creating base material model is explained.
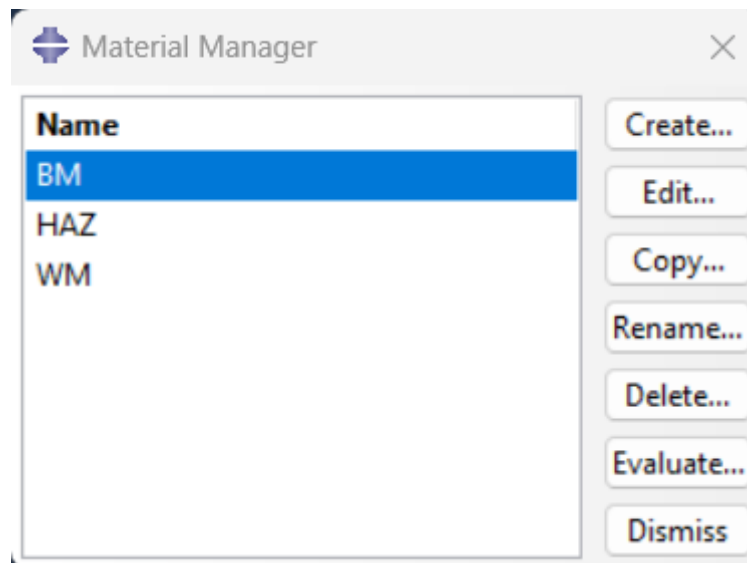
4. In **Mechanical** behavior choose **Damage for Ductile Metals**. Choose **Ductile Damage**. Input the calculated values responsible for the fracture behavior of the material (Fracture Strain, Stress Triaxiality, Strain Rate)
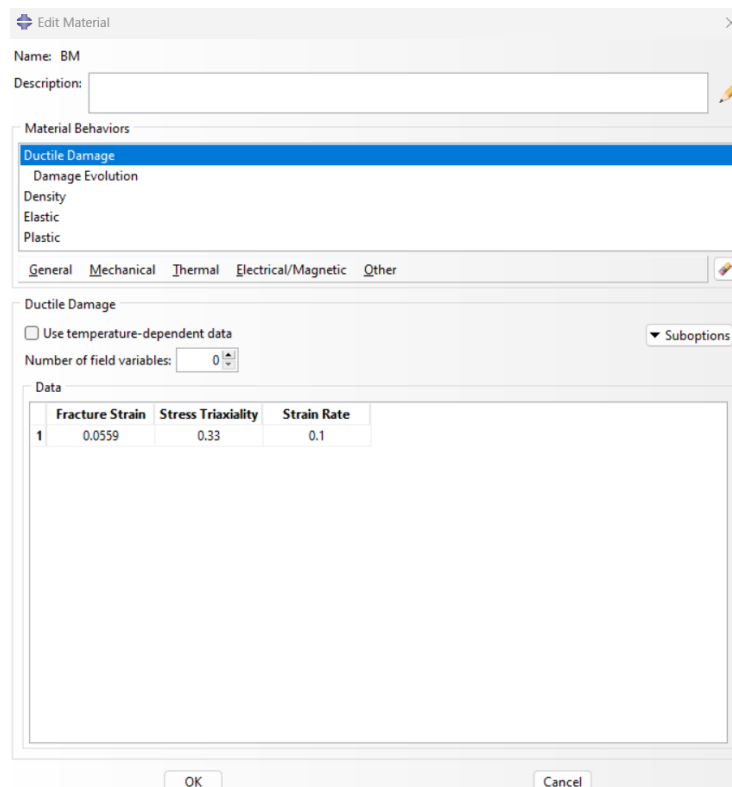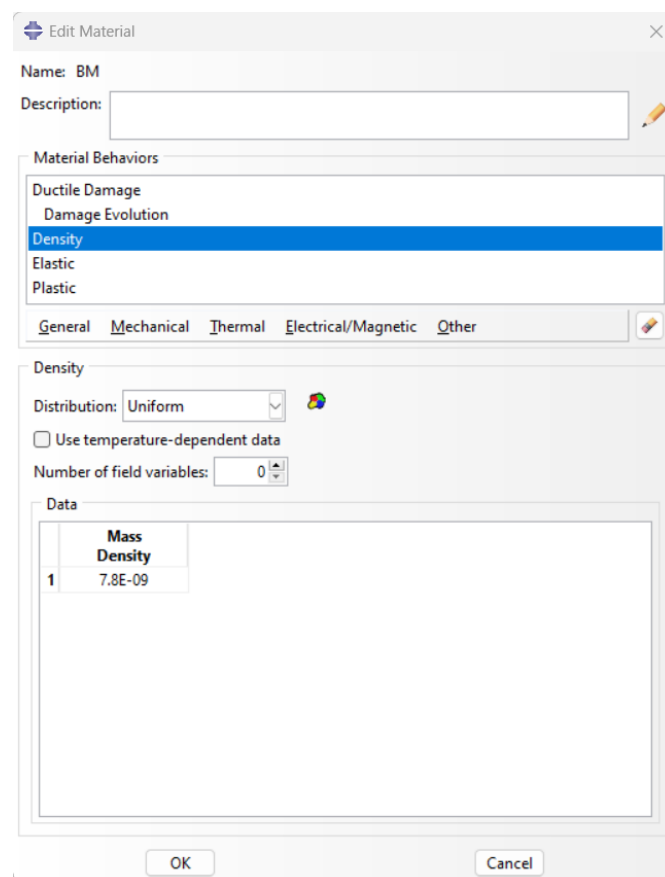
5. In the same behavior choose the sub option **Damage Evolution**. Define the type as **Energy**, softening as **Exponential** and input the value required for the fracture of the material.

6. **In General** behavior choose **Density** and input the mass density of the material.

7. In **Mechanical** behavior choose **Elasticity** and then **Elastic**. Specify the Modulus of Elasticity (E) and the Poisson's ratio (n)
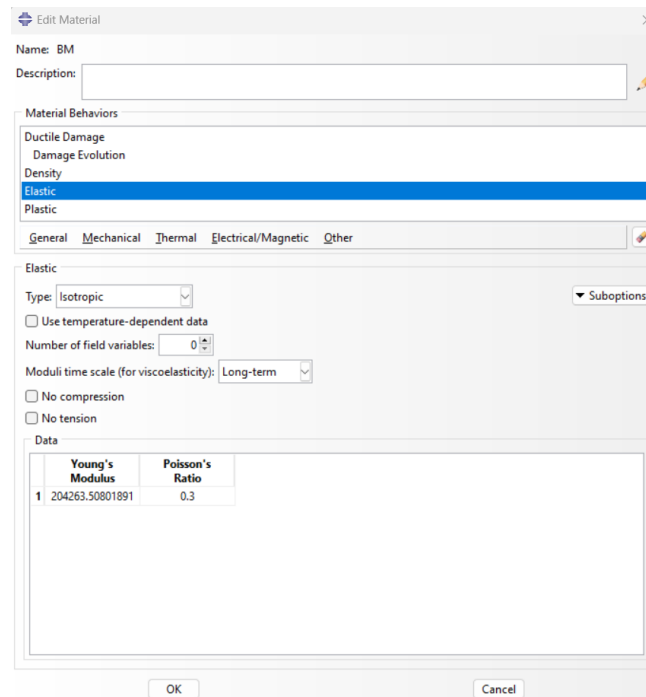

In the same tool tab choose Set to create a set around this reference point.
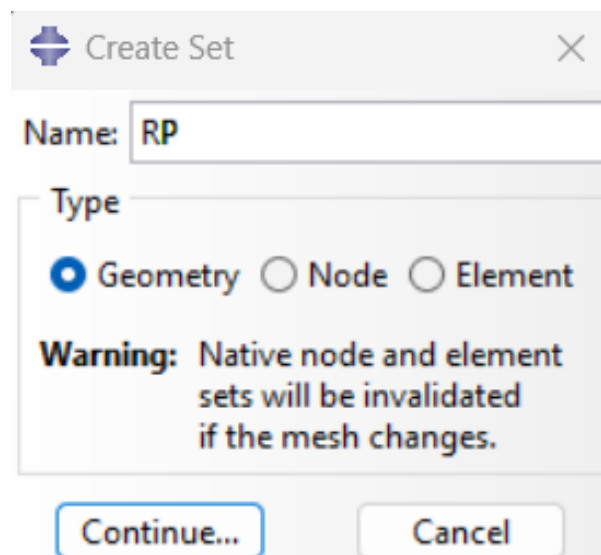
8. Go to **Step** Module. Open **Step Manager**. Create a new **Step** right after the **Initial** one. Choose Dynamic, Explicit.
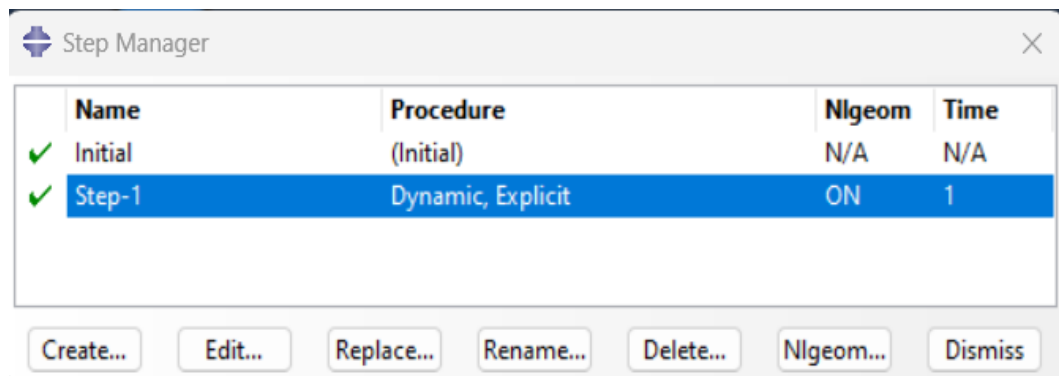

9. In **Step** Editing tool leave default values for the final simulation and change the step time to 0.1 second. However, while working on the model, it is recommended to use **Mass Scaling** to lower the computational times of the simulation. To do that create a scaling definition in the **Mass Scaling** tab. Specify the scaling factor as 100.
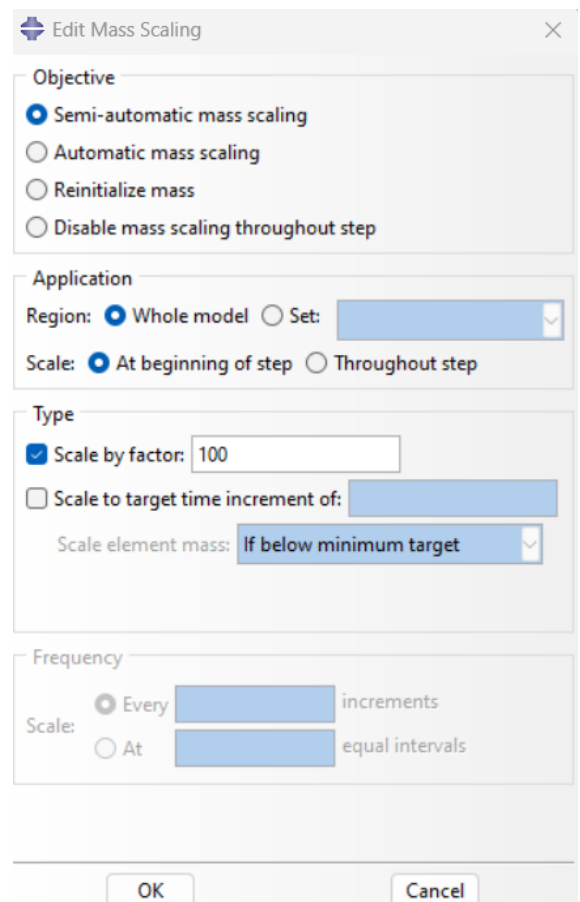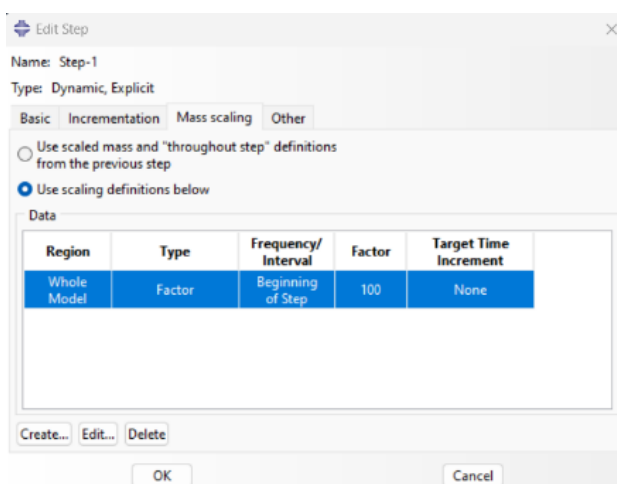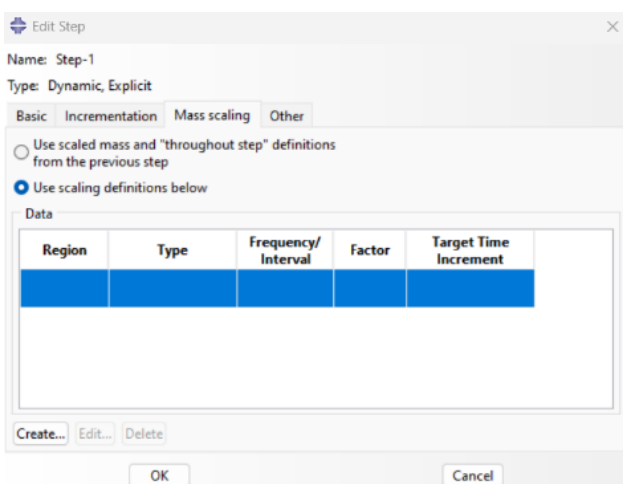
10. In the **Step** Module go to **History Output Requests** Manager. Delete the old history output request and create a new one. Concentrate the new request around previously created Set RP and choose output variables the RF2 (Force in y direction) and U2 (Displacement in y direction). This request is needed to create a force displacement graph after the simulation.
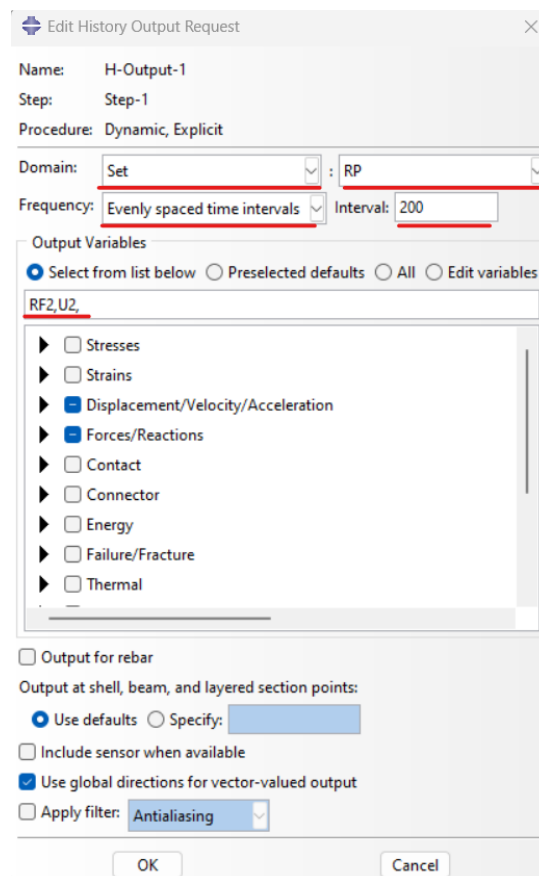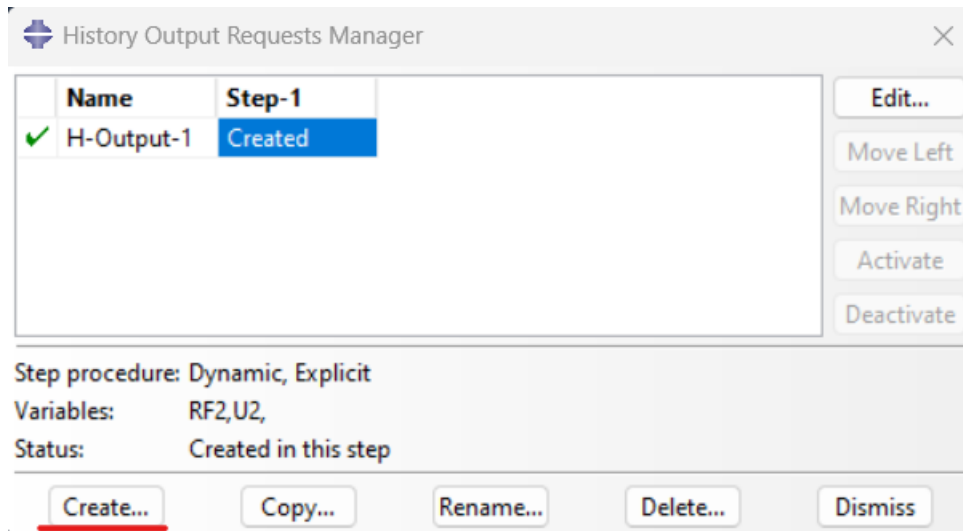
11. In the **Step** Module go to **Field Output Requests** Manager. Edit the request and add following output variables to the request. This request is needed to create a stress and strain graph after the simulation.
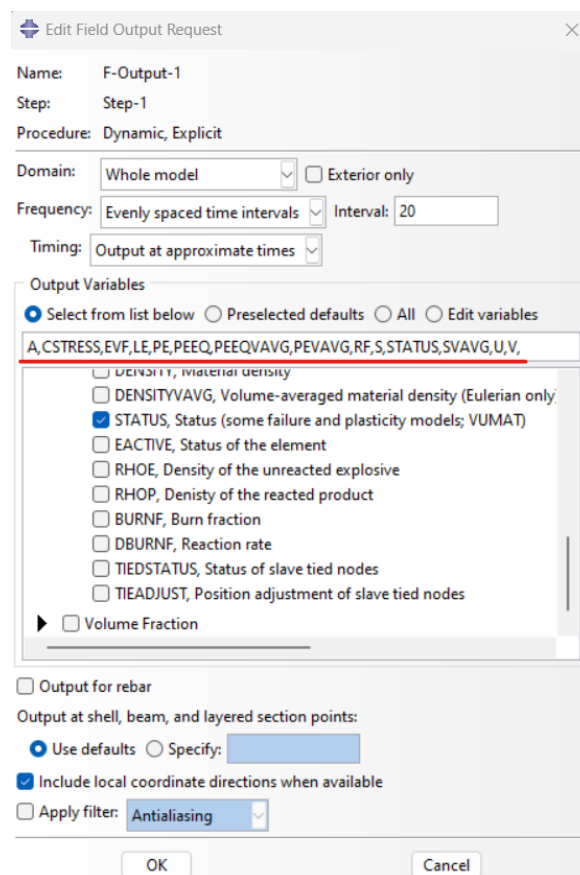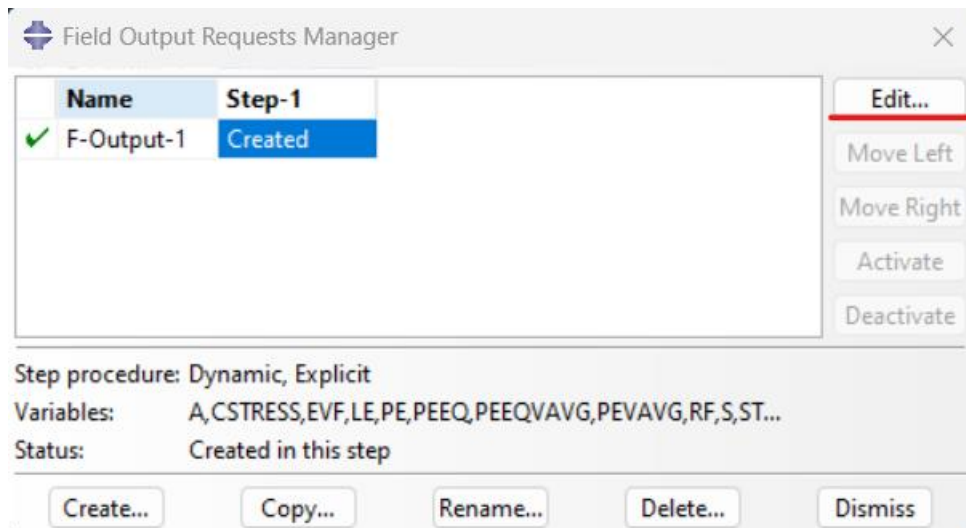
12. Go to **Interaction** Module and press **Create Constraint.** Create a **coupling constraint** and choose the reference point created before as a **constraint control point**. Choose **surface** as option for **constraint region type** and select the top surface of the crosshead. This way the crosshead cell of the model is fixed to the reference point and by pulling the reference point, the specimen will start stretching.
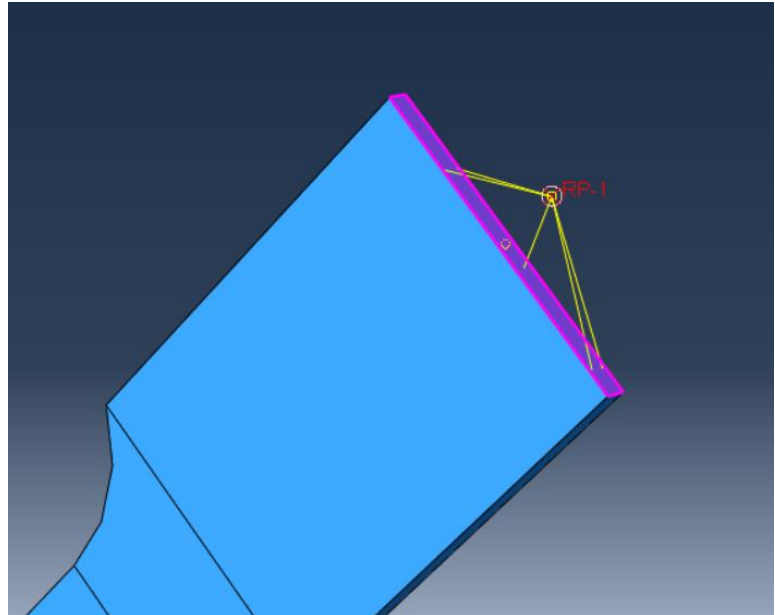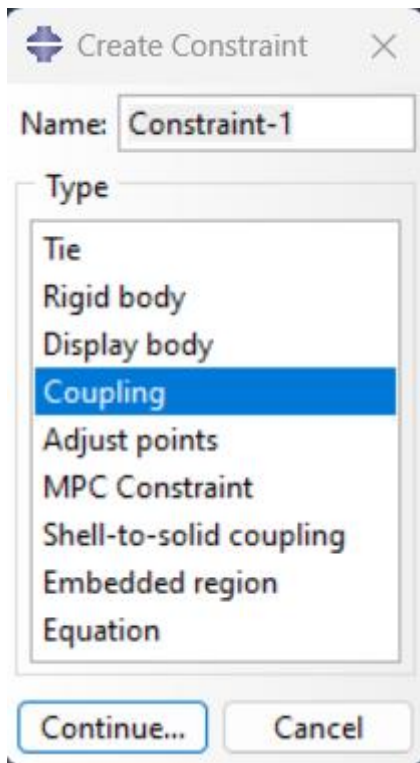
13. Go to **Load** Module. Press **Create Boundary Condition.** Choose Initial **Step** and Encastre to fix another crosshead of the specimen.
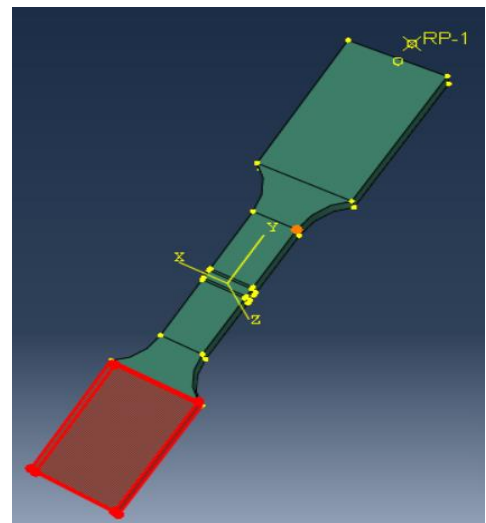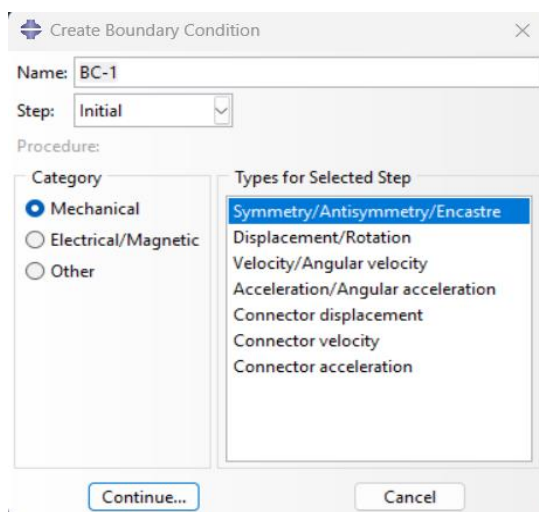
14. Create boundary condition and select the reference point as region for boundary condition. Choose Displacement/Rotation. Constrain the model in all directions except the axis along the direction of the tensile test.
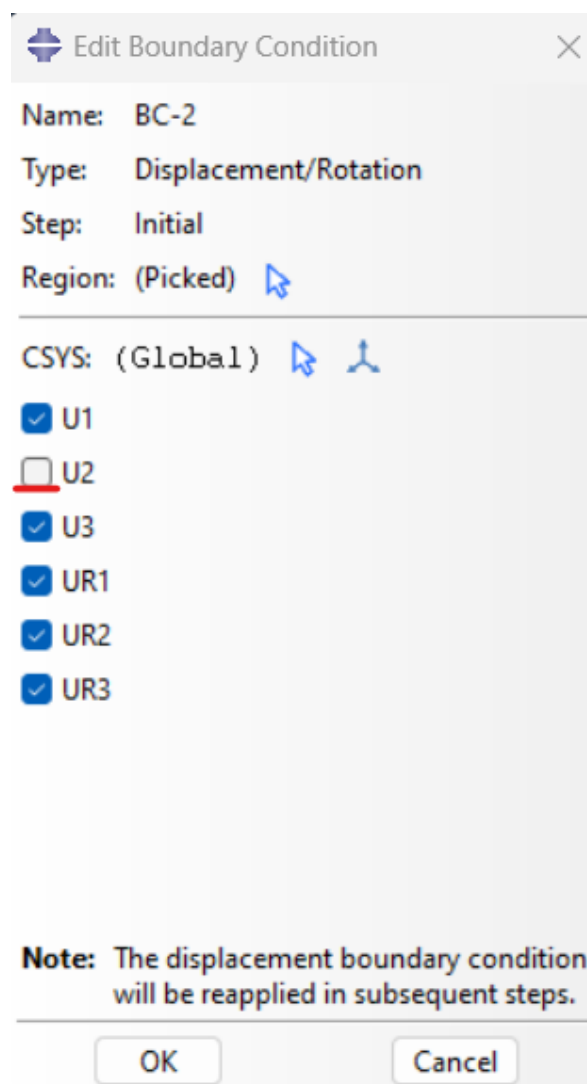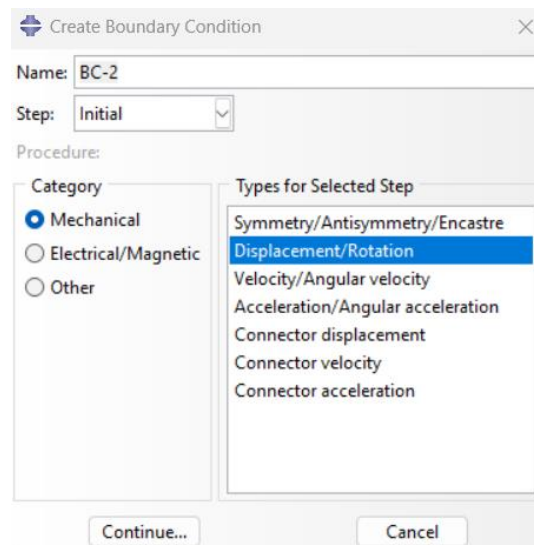
15. Create another boundary condition around the reference point and select Step-1 this time as the step, as this function will be responsible for the tension of the specimen during the simulation. Specify the displacement during the simulation in U2 field and create the amplitude for the applied load.

Edit Boundary Condition ✕

Name: BC-3
Type: Displacement/Rotation
Step: Step-1 (Dynamic, Explicit)
Region: (Picked)

CSYS: (Global)

Distribution: Uniform — f(x)

☐ U1:
☑ U2: 6.9
☐ U3:
☐ UR1: radians
☐ UR2: radians
☐ UR3: radians

Amplitude: Amp01

Note: The displacement boundary condition will be reapplied in subsequent steps.

OK   Cancel

The amplitude for the boundary condition:

Edit Amplitude	✕

Name: Amp01
Type: Tabular

Time span: Step time ⌄

Smoothing: ⦿ Use solver default
⃝ Specify: [____]

Amplitude Data   Baseline Correction

	Time/Frequency	Amplitude
1	0	0
2	0.0025	0.025
3	0.005	0.05
4	0.0075	0.075
5	0.01	0.1
6	0.0125	0.125
7	0.015	0.15
8	0.0175	0.175
9	0.02	0.2
10	0.0225	0.225
11	0.025	0.25
12	0.0275	0.275
13	0.03	0.3
14	0.0325	0.325
15	0.035	0.35
16	0.0375	0.375
17	0.04	0.4
18	0.0425	0.425
19	0.045	0.45
20	0.0475	0.475
21	0.05	0.5
22	0.0525	0.525
23	0.055	0.55
24	0.0575	0.575
25	0.06	0.6
26	0.0625	0.625
27	0.065	0.65
28	0.0675	0.675

OK   Cancel

Edit Amplitude	✕

Name: Amp01
Type: Tabular

Time span: Step time ⌄

Smoothing: ⦿ Use solver default
⃝ Specify: [____]

Amplitude Data   Baseline Correction

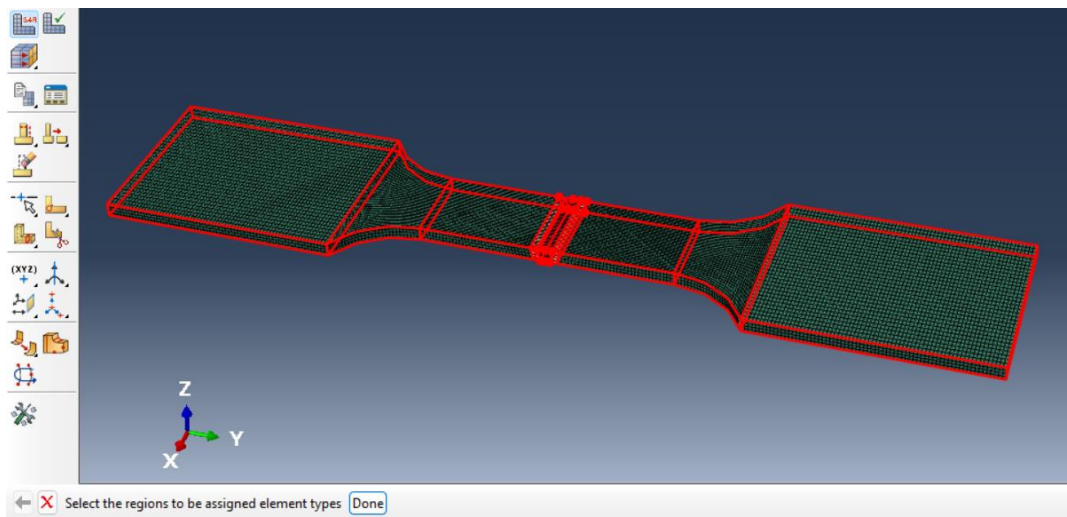|	Time/Frequency	Amplitude
14	0.0325	0.325
15	0.035	0.35
16	0.0375	0.375
17	0.04	0.4
18	0.0425	0.425
19	0.045	0.45
20	0.0475	0.475
21	0.05	0.5
22	0.0525	0.525
23	0.055	0.55
24	0.0575	0.575
25	0.06	0.6
26	0.0625	0.625
27	0.065	0.65
28	0.0675	0.675
29	0.07	0.7
30	0.0725	0.725
31	0.075	0.75
32	0.0775	0.775
33	0.08	0.8
34	0.0825	0.825
35	0.085	0.85
36	0.0875	0.875
37	0.09	0.9
38	0.0925	0.925
39	0.095	0.95
40	0.0975	0.975
41	0.1	1

OK   Cancel

16. Go to **Mesh** Module and press **Seed Part.** Then mesh the part with applied seeds. The example is the simplified coarse mesh to run the simulation faster.
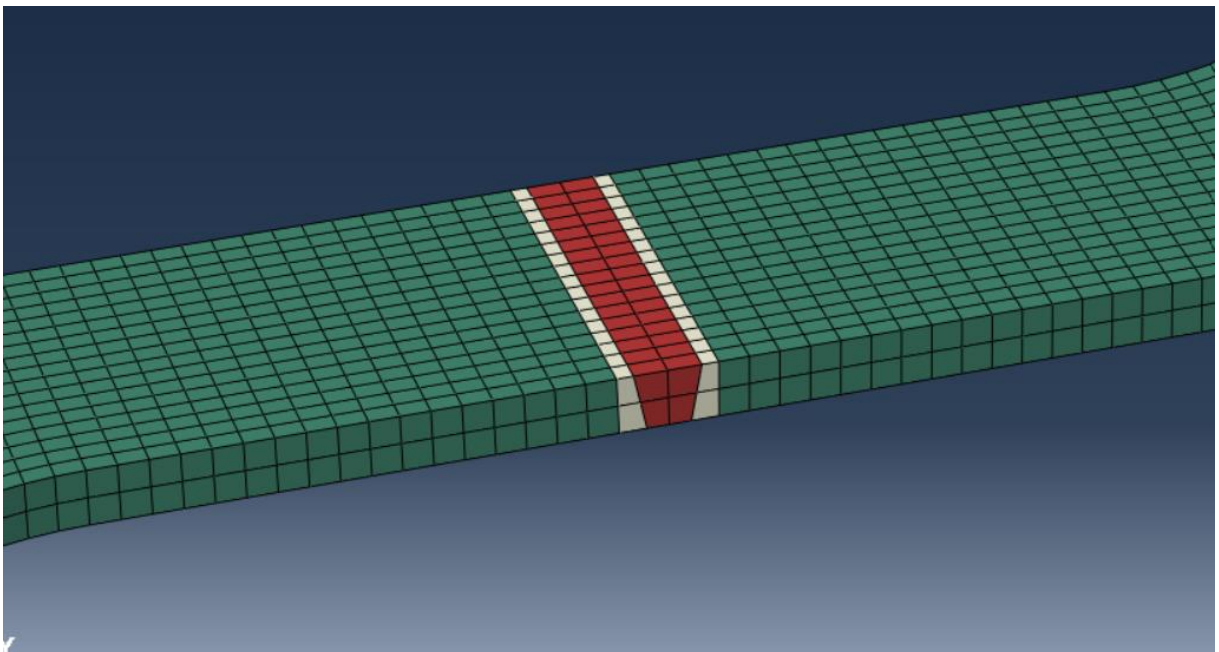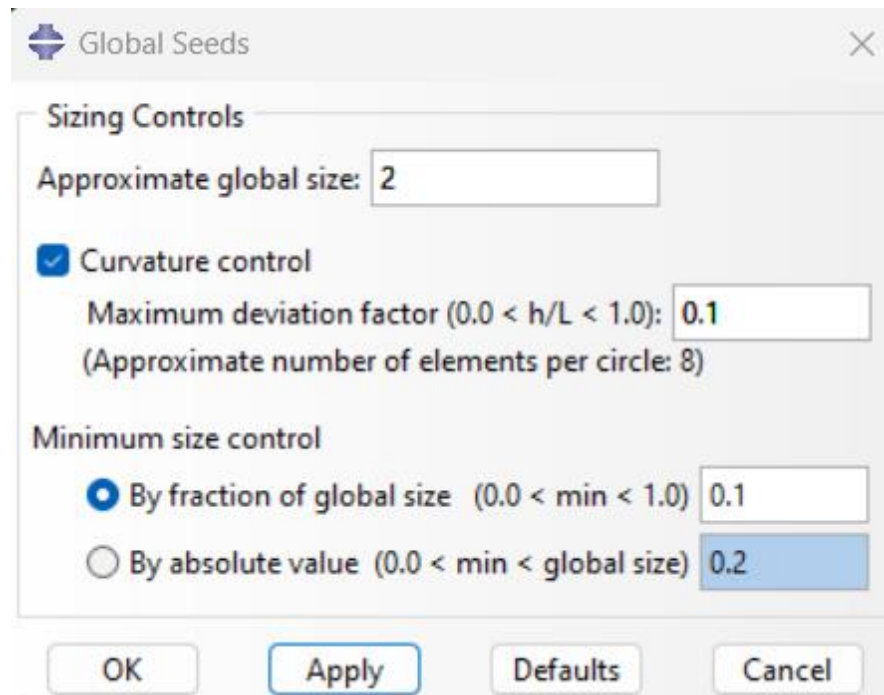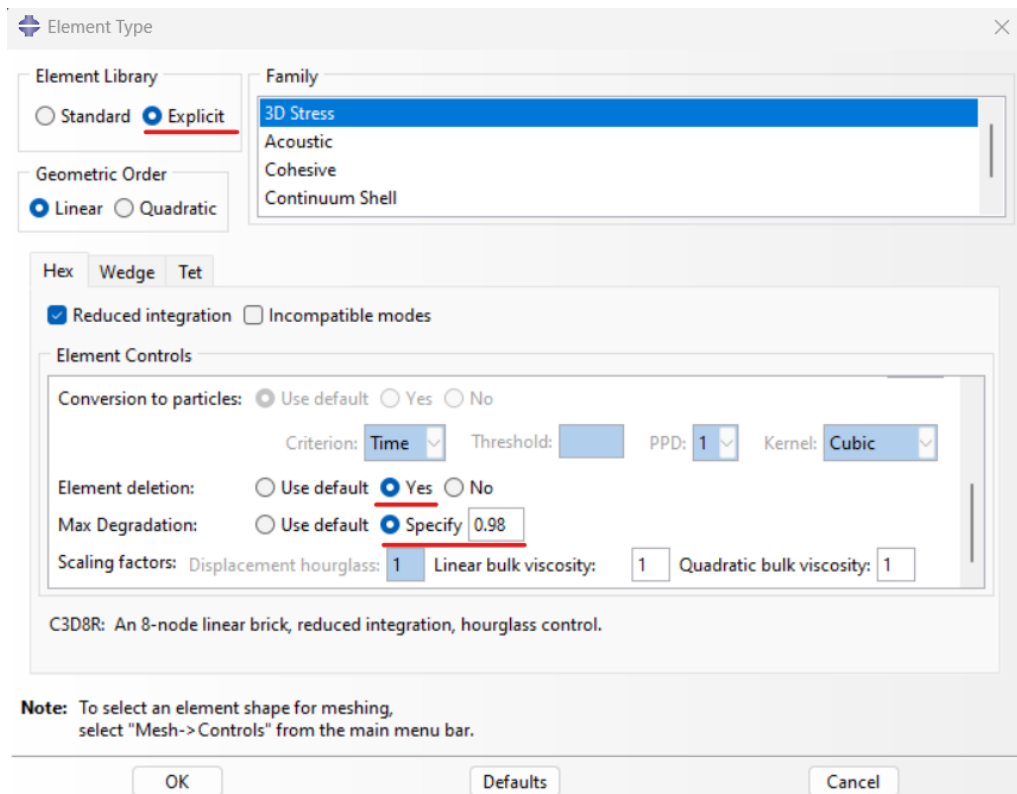
17. To create mesh for the final model, finer mesh is required. To do that, use **Seed Edges** tool and specify more elements per edge.
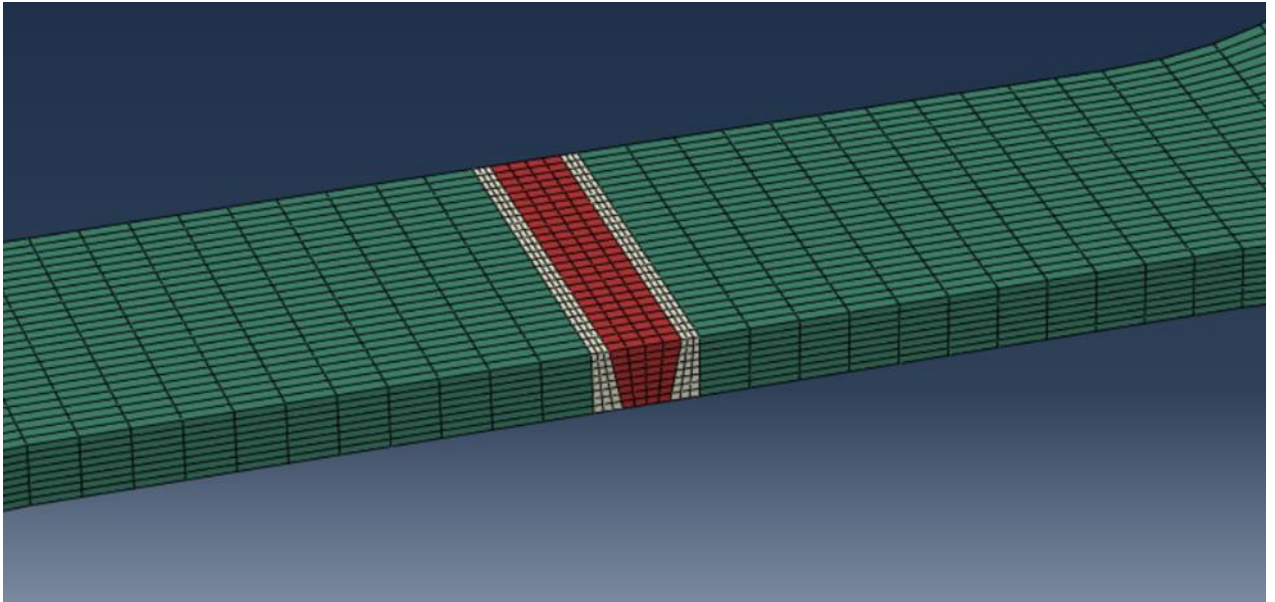
18. Choose **Assign Element Type** and select the whole model. In the menu selecting the Explicit and Element deletion options is crucial, as this way the model will break after fracture.

Appendix 2. Material input values

Elastic behavior. The same values are applied to each material

Density. The same values are applied to each material

Plastic behavior. HAZ, BM, WM

σ_{true}	ε_{pl}
724.6004	0
726.5411	0.000135
728.3689	0.000273
730.1527	0.000418
731.7887	0.000563
733.3452	0.000711
734.8206	0.000865
736.2345	0.001022
737.5301	0.001177
738.7915	0.001338
739.9881	0.001501
741.1814	0.001678
742.246	0.001847
743.2618	0.002017
744.2206	0.002186
745.1535	0.002359
746.0178	0.002533
747.3943	0.002826
747.7262	0.002902
748.4932	0.003081
752.9804	0.00333
761.6913	0.004565
768.5147	0.007283
777.6267	0.011207
789.7232	0.016655
803.2014	0.02336
815.9639	0.03084
828.7373	0.040515
838.5842	0.050285
847.9984	0.061663
856.915	0.074111
864.9317	0.087111
872.2691	0.100724
878.6841	0.114138
884.5394	0.127749
886.794	0.133367

σ_{true}	ε_{pl}
788.9741	0
791.0871	0.000135
793.0773	0.000273
795.0197	0.000418
796.8009	0.000563
798.4957	0.000711
800.1022	0.000865
801.6418	0.001022
803.0524	0.001177
804.4259	0.001338
805.7288	0.001501
807.0282	0.001678
808.1873	0.001847
809.2933	0.002017
810.3373	0.002186
811.3531	0.002359
812.2942	0.002533
813.793	0.002826
814.1544	0.002902
814.9895	0.003081
819.8753	0.00333
829.3601	0.004565
836.7897	0.007283
846.7112	0.011207
859.8824	0.016655
874.558	0.02336
888.4543	0.03084
902.3625	0.040515
913.0842	0.050285
923.3347	0.061663
933.0435	0.074111
941.7724	0.087111
949.7617	0.100724
956.7466	0.114138
963.1221	0.127749
965.5769	0.133367

σ_{true}	ε_{pl}
859.035	0
861.3357	0.000135
863.5026	0.000273
865.6174	0.000418
867.5568	0.000563
869.4022	0.000711
871.1513	0.000865
872.8276	0.001022
874.3635	0.001177
875.859	0.001338
877.2775	0.001501
878.6923	0.001678
879.9543	0.001847
881.1585	0.002017
882.2953	0.002186
883.4012	0.002359
884.4259	0.002533
886.0578	0.002826
886.4513	0.002902
887.3605	0.003081
892.6802	0.00333
903.0073	0.004565
911.0966	0.007283
921.8991	0.011207
936.24	0.016655
952.2188	0.02336
967.3491	0.03084
982.4923	0.040515
994.1661	0.050285
1005.327	0.061663
1015.898	0.074111
1025.402	0.087111
1034.1	0.100724
1041.706	0.114138
1048.647	0.127749
1051.32	0.133367

Ductile Damage. The same values are applied to each material

Edit Material   ✕

Name: BM

Description: [   ] ✏

Material Behaviors

Ductile Damage
Damage Evolution
Density
Elastic
Plastic

General   Mechanical   Thermal   Electrical/Magnetic   Other   ✏

Ductile Damage

☐ Use temperature-dependent data   ▼ Suboptions

Number of field variables: 0 ⇕

Data

	Fracture Strain	Stress Triaxiality	Strain Rate
1	0.0559	0.33	0.1

OK   Cancel

Damage Evolution. BM

Damage Evolution. HAZ

Damage Evolution. WM